CR 179572
SAIC 87/1612

MASS FLOW METER USING THE TRIBOELECTRIC EFFECT FOR MEASUREMENT IN CRYOGENICS

NASA CONTRACT NAS324648

Final Report

April, 1987

Prepared for:

NASA-LEWIS RESEARCH CENTER

CLEVELAND, OH 44135

By:

Henry Bernatowicz

Jock Cunningham

Steve Wolff

Prepared by:

Science Applications International Corporation

1257 Tasman Dr.

Sunnyvale, CA 94089

1. Report No.	2. Government Accession No.	3. Recipient's Catalog No.
CR 179572		

4. Title and Subtitle	5. Report Date
MASS FLOW METER USING THE TRIBOELECTRIC EFFECT FOR MEASUREMENT IN CRYOGENICS	6. Performing Organization Code: 525-02-19

7. Author(s)	8. Performing Organization Report No.
Henry Bernatowicz Jock Cunningham Steve Wolff	10. Work Unit No.

9. Performing Organization Name and Address	11. Contract or Grant No.
SCIENCE APPLICATIONS INTERNATIONAL CORPORATION 1257 Tasman Drive Sunnyvale, CA 94089	NAS 3-24648
	13. Type of Report and Period Covered: Final 12-86
12. Sponsoring Agency Name and Address	14. Sponsoring Agency Code
NATIONAL AERONAUTICS AND SPACE ADMINISTRATION Washington, D.C. 20546	

15. Supplementary Notes

R.M. Masters, Project Manager
NASA Lewis Research Center
Cleveland, OH 44135

16. Abstract

The technique of using triboelectric charge to measure the mass flow rate of cryogens for the Space Shuttle Main Engine was investigated. Cross correlation of the triboelectric charge signals was used to determine the transit time of the cryogen between two sensor locations in a 3/4 inch tube.

The ring electrode sensors were mounted in a removable spool piece. Three spool pieces were constructed for delivery, each with a different design. One set of electronics for implementation of the cross correlation and flow calculation was constructed for delivery.

Tests were made using a laboratory flow loop using liquid freon and transformer oil. The measured flow precision was 1% and the response was linear. The natural frequency distribution of the triboelectric signal was approximately 1/f. The sensor electrodes should have an axial length less than approximately one tenth pipe diameter. The electrode spacing should be less than approximately one pip diameter.

Tests using liquid nitrogen demonstrated poor tribo-signal to noise ratio. Most of the noise was microphonic and common to both electrode systems. The common noise rejection facility of the correlator was successful in compensating for this noise but the signal was still too small to enable reliable demonstration of the technique in liquid nitrogen.

17. Key Words (Suggested by Author(s))	18. Distribution Statement
Transducer - Flow-Cryogenic Transducer - Triboelectric Effect Transducer - Flow Non-Intrusive	

19. Security Classif. (of this report)	20. Security Classif. (of this page)	21. No. of pages	22. Price*
Unclassified	Unclassified		

*For sale by the National Technical Information Service, Springfield, Virginia 22161

TABLE OF CONTENTS

TABLE OF CONTENTS

LIST OF FIGURES

LIST OF FIGURES

LIST OF PLATES

LIST OF TABLES

FORWARD

This work was done under NASA contract NAS3-24648. It is among the first known attempts to apply cross correlation techniques to the measurement of cryogenic flow using the triboelectric effect.

Special assistance was given by George Rossman who made the facilities of American Welding available for testing of the flow meters with liquid nitrogen.

Appreciation is also expressed for assistance given by Dr. David Dekker of Mount Isa Mines Limited (Australia), who developed the common mode rejection cross correlator circuit.

ABSTRACT

The technique of using triboelectric charge to measure the mass flow rate of cryogens for the Space shuttle Main Engine was investigated. Cross correlation of the triboelectric charge signals was used to determine the transit time of the cryogen between two sensor locations in a 3/4 inch tube.

The ring electrode sensors were mounted in a removable spool piece. Three spool pieces were constructed for delivery, each with a different design. One set of electronics for implementation of the cross correlation and flow calculation was constructed for delivery.

Tests were made using a laboratory flow loop using liquid freon and transformer oil. The measured flow precision was 1% and the response was linear. The natural frequency distribution of the triboelectric signal was approximately 1/f. The sensor electrodes should have an axial length less than approximately one tenth pipe diameter. The electrode spacing should be less than approximately one pip diameter.

Tests using liquid nitrogen demonstrated poor tribo-signal to noise ratio. Most of the noise was microphonic and common to both electrode systems. The common mode noise rejection facility of the correlator was successful in compensating for this noise but the signal was still too small to enable reliable demonstration of the technique in liquid nitrogen.

1.0 SUMMARY

The objectives of this contract was to develop, test and deliver three flow meter spool piece designs for measuring LOX and LH_2. The intended application was for the Space Shuttle Main Engine (SSME) test stand.

Liquid freon, water and transformer oil were used to develop the spool pieces. All spool pieces worked well and confirmed general understanding of the technique. Flow rate precision of approximately 1% was measured and the response was linear. Electrode geometry should have short (axially) electrodes ($\leq$ one tenth of the pipe diameter). The electrodes should be spaced close together ($\leq$ 1 pipe diameter) and the frequency response of the electronics should have a lower limit above the reciprocal of the transit time. The natural frequency distribution of the signal is approximately $1/f$.

Tests with liquid nitrogen showed large amounts of microphonic noise common to both electrodes. The common mode noise rejection facility of the correlator compensated adequately for this.

2.0 INTRODUCTION

Currently fuel flow rates within the Space Shuttle Main Engine (SSME) are measured with a turbine type instrument that has a forward pressure drop. For turbine flow meters there are credible failure modes that could result in engine damage. This is always a risk for intrusive devices. This project is to develop a flow meter that is nonintrusive and does not result in a pressure drop.

For some time, the use of cross correlation in flow measurement has been investigated. Only in the last 5 to 8 years has the technique become practical because of the availability of customized solid state electronics on an affordable scale. Before this, experimental arrangements were constructed using computers or very simple hardware circuits. These circuits were slow and inefficient and the former required expensive computers to be fast and efficient.

TRW developed an integrated circuit to carry out the cross correlation of two signals in digital (single bit) form. This lowers the computational overhead required by computers. The chip was designed primarily for radar and sonar signal processing where return signals can be cross correlated with transmitted signals for identification. This chip has made it possible to build a full cross correlator on a double sided circuit board measuring only 187 X 229 mm. Among many features, the circuit based on the TRW chip provides a signal directly proportional to velocity, correlation display functions (for an oscilloscope) and a common mode rejection facility.

Future developments in electronics will provide for further reduction in correlator size and chip count. Programmable gate arrays are available now that can incorporate digital circuits on a single chip. The TRW based correlator circuit is currently being converted to take advantage of this. Hence, the use of cross correlation for flow measurement will become more wide spread in the near future.

Cross correlation requires a (natural) flow derived signal to be detected at a point along the flow path. This effectively labels the particular fluid segment. A similar signal is also obtained from a second location, a short distance down stream. The two signals are cross correlated to determine the transit time for the naturally labeled segment to arrive at the down stream location. The inverse of the transit time, multiplied by the separation between the two locations yields the flow velocity.

Generally the source of a signal takes different forms depending on the application. Where large density fluctuations occur in turbulent streams, a density sensitive measurement can be made at two locations to provide a signal. Where large capacitive changes occur, capacitive sensors can be used. There are many examples of sensors that can be used.

Considerable experience has been gained by the contractor with the use of triboelectric charge applied to two phase flow measurement. From the literature such charge has been detected in water, hydrocarbon fuels and liquid nitrogen and helium. The use of charge is appropriate technology for the SSME because of the large amount of turbulence induced by turbocompressors and because the charge sensing electrodes can be mounted unobtrusively in the wall of the flow duct. No indication is available in the literature as to the amount of charge generated under particular circumstances.

Successful development of this technique for the extreme environment conditions of the SSME will present a new generation of flow meters for cryogenic applications in particular and accelerate the general application to industry.

This contract required the development, testing and delivery of three flow meter spool piece designs. The flow meters used triboelectric charge coupled with cross correlation to determine accurate cryogenic flow rate. These triboelectric flow meters (TEFM) were tested in liquid nitrogen with modest flow rates to indicate the feasibility of the technique. Consideration was given to the applicability of these tests to the intended final application.

3.0 TEFM PRINCIPLE OF OPERATION

3.1 Triboelectric Charge

Triboelectric charge is generated on objects that come in contact and rub against each other. The charge generation is caused by friction. Usually the two objects are composed of dissimilar materials, however on rare occasions charge can be generated by identical materials with asymmetric rubbing[1].

The phenomenon has been investigated and used for a considerable time, however no theoretical or quantitative explanation has been developed. Thus, prediction of the amount of charge generated under known circumstances relies on an empirical relationship developed after a great deal of experimentation. The effects of charging ones body through walking on a carpet is well known.

Studies[2][1] of the process commonly result in a list of materials graded in order of their potential for charge generation (i.e., a triboelectric series). Charge generation can occur between any combination of those materials. The TEFM relies on charge generation between a liquid (liquid H_2, O_2, or N_2) and a solid (pipe or container walls). A common example of such charge results when hydrocarbon fuels flow through fuel lines and filters. This effect is of great importance to the aeronautical industry since a large accumulation of charge can cause sparking and fire or explosions. Studies of this application have been made[2][3].

The generation of charge by cryogenic fluids is not well covered in the literature. Static charge generation by liquid nitrogen passing from a dewar to a cryostat has been reported[4]. Artificial charging of liquid helium has also been investigated[5]. For all of these cases no mention is made of the ac component of this charge while the liquid is flowing.

The TEFM requires the detection of a small ac triboelectric signal. This results mainly from turbulent variations in the flow close to the pipe wall which are then mixed throughout the volume. Because the fluid of interest is

a poor electrical conductor this charge persists to label the fluid eddies. There is also a possibility that charge is generated from liquid-liquid contact away from the pipe wall.

The dc component is known as the streaming potential and its use for flow determination has been examined[6], however this technique requires a consistent measurement of the streaming potential magnitude. Such a measurement is difficult to make and is highly dependant on experimental conditions such as contamination and minor drifts in high impedance electronic circuits.

The effect of conductivity is also not well understood. One study[2] shows how the charging current for a fluid flowing through a platinum capillary varies with conductivity and Reynolds number. The current reaches a maximum as conductivity is increased but then decreases again at higher conductivities. The maximum occurs at different conductivities depending on the Reynolds number.

Hence, the generation of a suitable charge in cryogens can only be studied through experimentation. A high level of turbulence and liquid-metal friction is required and both of these requirements are met in the space shuttle main engine.

3.2 Flow Rate Measurement-Cross Correlation

Flow speed is determined by a transit time technique based on timing the delay in the triboelectric charge signal (ac) between two electrodes in the pipe wall. The two signals from the electrodes are cross correlated to determine the time delay.

Figure 3.1 shows an example of two triboelectric signals from flowing freon in a 3/4" diameter pipe. The time delay between them is apparent.

This technique has been investigated for some time and a summary of recent literature is given by Coulthard[7]. The technology used in this contract

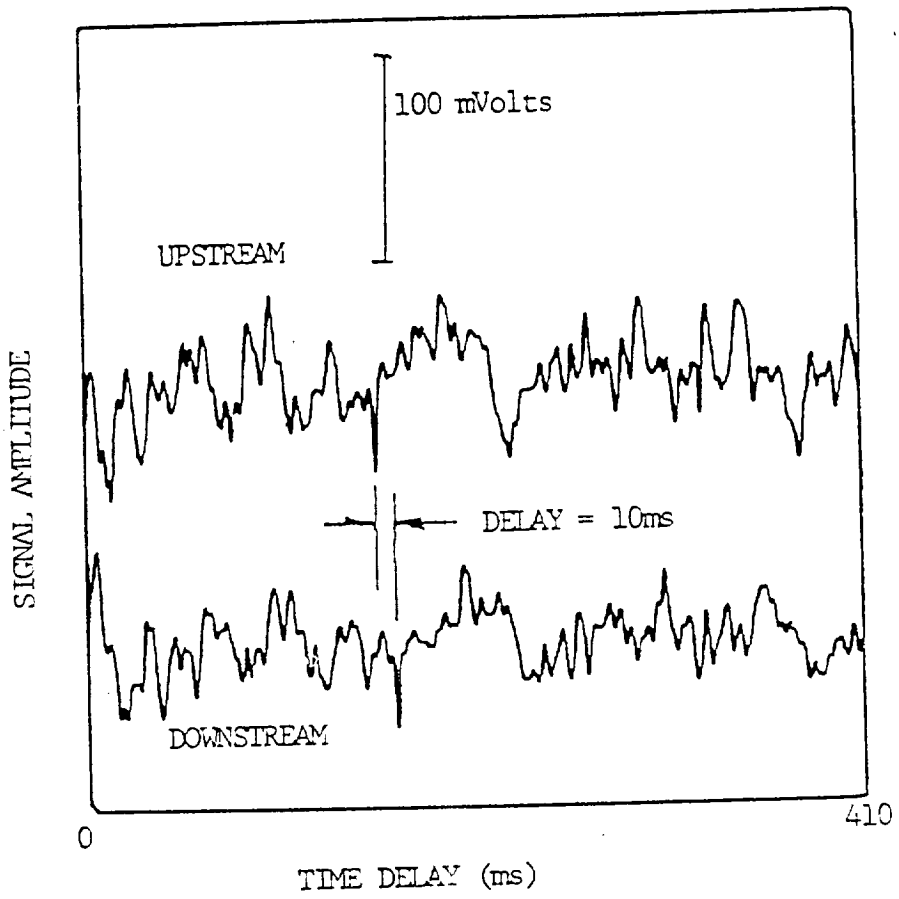

Figure 3.1

EXAMPLE OF TRIBOELECTRIC SIGNALS FROM TWO ELECTRODES SHOWING THE TRANSIT TIME DELAY

was developed from the application to the measurement of particulate mass flow[8-12]. Other applications of cross correlation have been examined by Bendat and Piersol[13].

Several means for deriving a flow sensitive a signal include: pressure fluctuations, ultrasonic and ionizing radiation attenuation, capacitance and triboelectric charge. These suit a wide range of applications.

3.2.1 Determination of Time Delay

The analog cross correlation function (R_{ud}) between an upstream signal U(t) and a downstream signal D(t) is defined as:

$$R_{ud}(\tau) = \lim_{T\to\infty} \frac{1}{T} \int_0^T U(t - \tau)\, D(t)dt \qquad (2)$$

where T is the integration (or measurement) time, t is the sample time, and is the time delay between the two signals. If $R_{ud}(\tau)$ is calculated over a continuous range of time delays , the transport time of the flowing material is the value of τ for which $R_{ud}(\tau)$ is a maximum. Since calculating this integral in an analog form requires high speed processing using a computer, the polarity cross correlation function is used. This reduces the amount of data required for analysis since the signal is only a single bit.

The digital or polarity cross correlation function C(j) is defined as:

$$C(j) = 1/N \sum_{i=1}^{N} U[-(i + j)\Delta t]\, D(-i\Delta t) \qquad (3)$$

where j is the time delay increment (Δt) number and U and D are the up and downstream signals, respectively. The function is averaged over N measurements and the delay time is equal to the correlation delay for which C(j) is a maximum.

Use of the digital correlation function does not alter the estimated value of the delay, however it does change the shape of the correlation peak, making it broader. To compensate for this, the smoothing or integration time may be increased to maintain precision in the estimate of time delay.

3.2.2 Precision and Resolution

The use of more bits of resolution in digitizing the signals improves the resolution but adds greatly to the processing overhead. It has been shown [14] that by using a two bit instead of a single bit conversion the signal to noise ratio can be halved. Only an extra 20% improvement can be achieved by going to 4 bit conversion which is effectively equivalent to analog correlation.

Thus the use of single bit correlation allows relatively simple electronics capable of operating at fast rates. The correlator circuit used for this contract is, however, capable of performing a two bit cross correlation.

The precision determining the time delay is related to the width of the peak in the cross correlation function. The width is in turn dependant upon the cross spectral bandwidth (B), the smoothing or integration time (T) and the normalized magnitude of the peak(R). Hence, the precision (σ) of the polarity correlation is given by:

$$\sigma = \sqrt{\frac{.033}{BT^2}\left\{2 - 1/R\right\}}$$

The precision is improved by increasing the cross spectral bandwidth, increasing the integration time and improving the degree of correlation. The latter (R) is normalized between 0 and 1 where 0.5 represents random, uncorrelated signal for a polarity (1 bit) correlator.

The relative measurement of the precision can be obtained by measuring the width of the cross correlation peak at half its maximum height (FWHM).

An indication of the effective bandwidth of the polarity signals can be obtained by obtaining the auto correlation function of one of the signals. The auto correlation function of a random period polarity function is represented by an exponential function with a decay time constant equal to the average rate of zero crossing.

Increasing the polarity bandwidth can be achieved by "whitening" the frequency spectrum. This is the case for the TEFM since most of the signal strength appears in the low frequency end of the spectrum. The low frequencies dominate the operation of the zero crossing converters. By reducing the amount of low frequency signal, the higher frequencies have more influence. Ideally the spectral content of the noise should be uniform.

Resolution in terms of the processing time delay increment T must be kept well within the precision of the correlation peak. Normally this not a problem and is easily achieved. When this condition is met, normal statistical variations in the location of the peak smooth out the incremental changes caused by T, a simple low pass filter on the output of the correlator is required.

3.2.3 Common Mode Compensation

A TEFM if used in the SSME would measure a great deal of interfering noise due to vibration of the high impedance electrode system. Most of this noise is expected (and verified in this work) to be common to both electrode channels (i.e., common mode noise - CMN).

Common mode noise rejection (CMR) is an essential feature of the correlator used in this contract. Figure 3.2 illustrates the effect of CMN ($R_{nn}(t)$) on the cross correlation function $R_{ud}(T)$ for two signals u(t) and d(t). The cross correlation function of CMN is essentially an auto correlation function which is symmetrical in positive and negative time and is periodic (depending on bandwidth). The signals u(t) and d(t) lead to a cross correlation function that is not symmetric in time and this property is used for CMR. The presence of CMN can bias the location of the cross correlation peak or

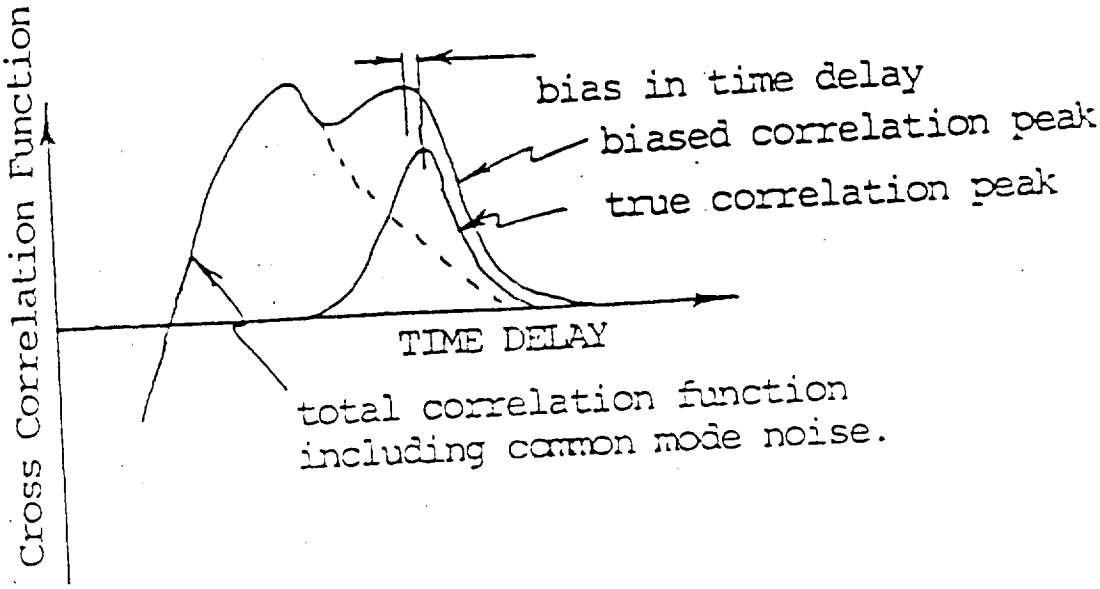

Figure 3.2

EFFECT OF THE COMMON MODE NOISE ON THE
CROSS CORRELATION FUNCTION

mask it completely. Examples of this and the operation of CMR are given in section 7.3.

Essentially, in terms of CMN, the correlator determines the negative time delay correlation function and subtracts it from the normal positive time delay function which removes the common mode or "auto correlation" component. It does this by alternately swapping the input signals. The negative correlation of true time delayed (positive) signals produces a featureless correlation function.

Considering the cross correlation function $R_{yx}(T)$ of two signals y(t) and x(t) given by

$$R_{yx}(T) = \frac{1}{M}\int_{o}^{M} y(t)\, x\,(t-T)\, dt$$

where T is the delay time between the signals and M is the total sampling time. If y(t) is the output of a linear system with input x(t) and impulse response h(T) then the following convolution relation holds:

$$R_{yx}(T) = \int_{o}^{\infty} h\,(T-t)\, R_{xx}(t)\, dt$$

where R_{xx} is the auto correlation of x(t) when noise n(t) is added and when there is a pure transport delay (L), h(T) becomes a unit impulse at time delay L and

$$R_{yx}(T) = R_{xx}\,(T-L) + R_{nn}\,(T)$$

Since all auto correlations including $R_{nn}(T)$, are symmetrical about T = 0 then

$$R_{nn}\,(T) = R_{nn}\,(-T)$$

and

$$R_{yx}(T) - R_{yx}\,(-T) = R_{xx}\,(T-L) - R_{xx}\,(-T-L)$$

In order to determine L accurately, the signals x(t) and y(t) must have a bandwidth sufficient to ensure that h(T) is a narrow peak at lag time L, and thus that $R_{xx}(T)$ is very small for $|T| > L$ and therefore

$$R_{yx}(T) - R_{yx}(-T) = R_{xx}(T-L)$$

is the cross correlation free from noise n(t).

4.0 SPOOL PIECE DESIGN

4.1 Design Overview

Three spool piece designs were fabricated and tested to determine the effects of electrode axial length and electrode spacing. Figures 4.1 to 4.3 show mechanical details of designs-A, B and C respectively while Plate 4.1 shows a photograph of design-C assembled with the preamplifier.

The spool pieces are based on a 19.05 mm diameter stainless steel tube with ring electrodes (brass) mounted flush in the tube wall. The electrodes are insulated from the tube by teflon insulators that also serve as seals. The spool piece is constructed in three basic sections (MK1, MK2, MK3) that bolt together with six 1/4" stainless steel bolts. The middle section contains the electrodes and feed-through wires while the two ends contain 3/4" pipe threads for coupling into the flow loop.

The enclosure containing the preamplifier circuit mounts above the electrode connection exits on brackets attached to two of the 6 assembly bolts. Electrode connecting wires pass through stainless steel tubes (nipples) screwed into the spool piece around the wire exit holes. These tubes lead into the preamplifier box providing mechanical support and shielding from electromagnetic interference. The tubes are also insulated from the preamplifier enclosure to minimize cooling of the preamplifier circuit. This also eliminates the potential for electrical interference by earth loops. The "ground" connection path runs from the spool piece body to the preamplifier enclosure via the support brackets.

Provision is made to heat the preamplifier enclosure with heating tapes and to purge it with dry nitrogen gas. This prevents cooling of the circuit and condensation of moisture about the high impedance parts of the circuit board.

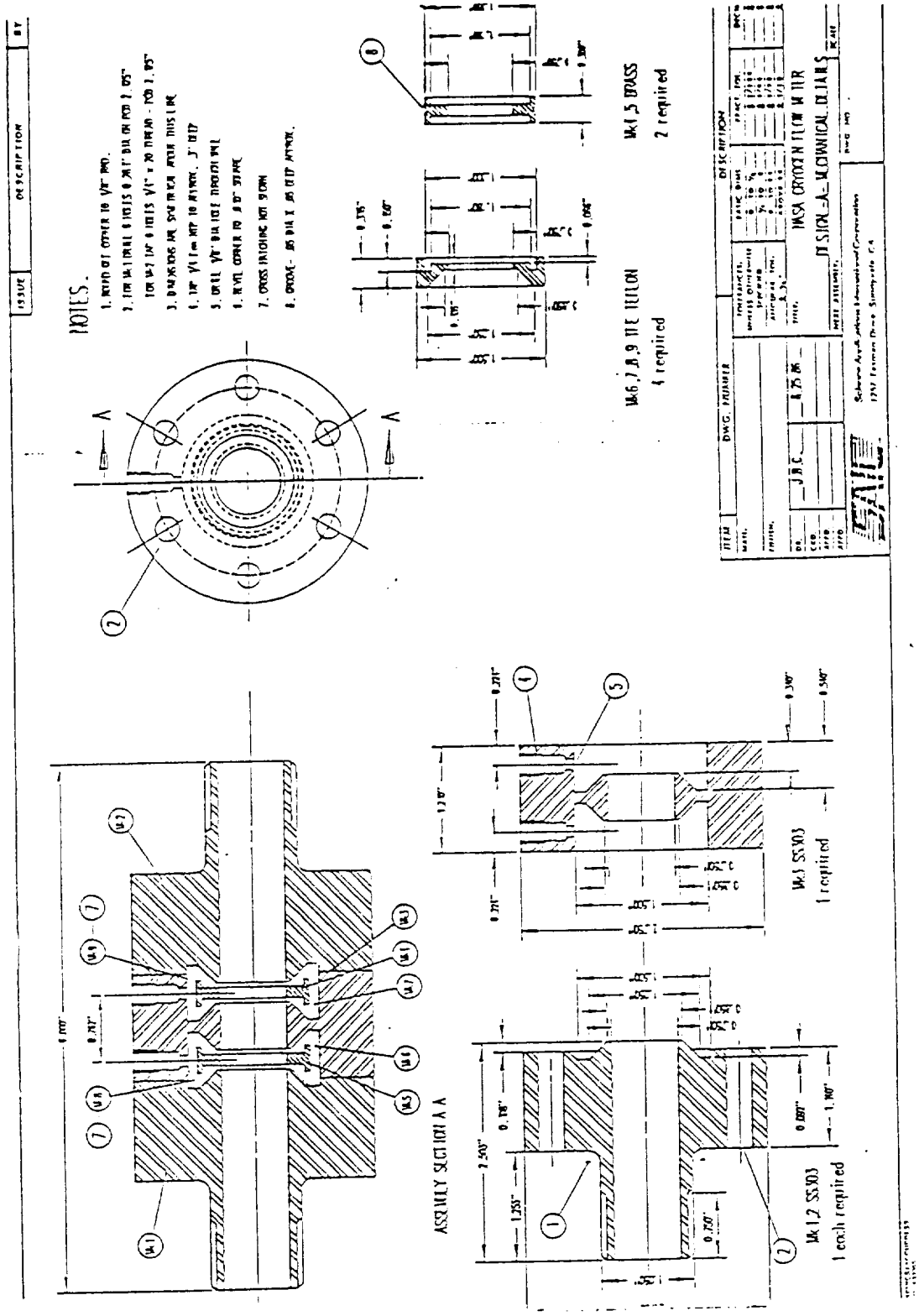

Figure 4.1

MECHANICAL DETAILS OF THE SPOOL PIECE DESIGN-A

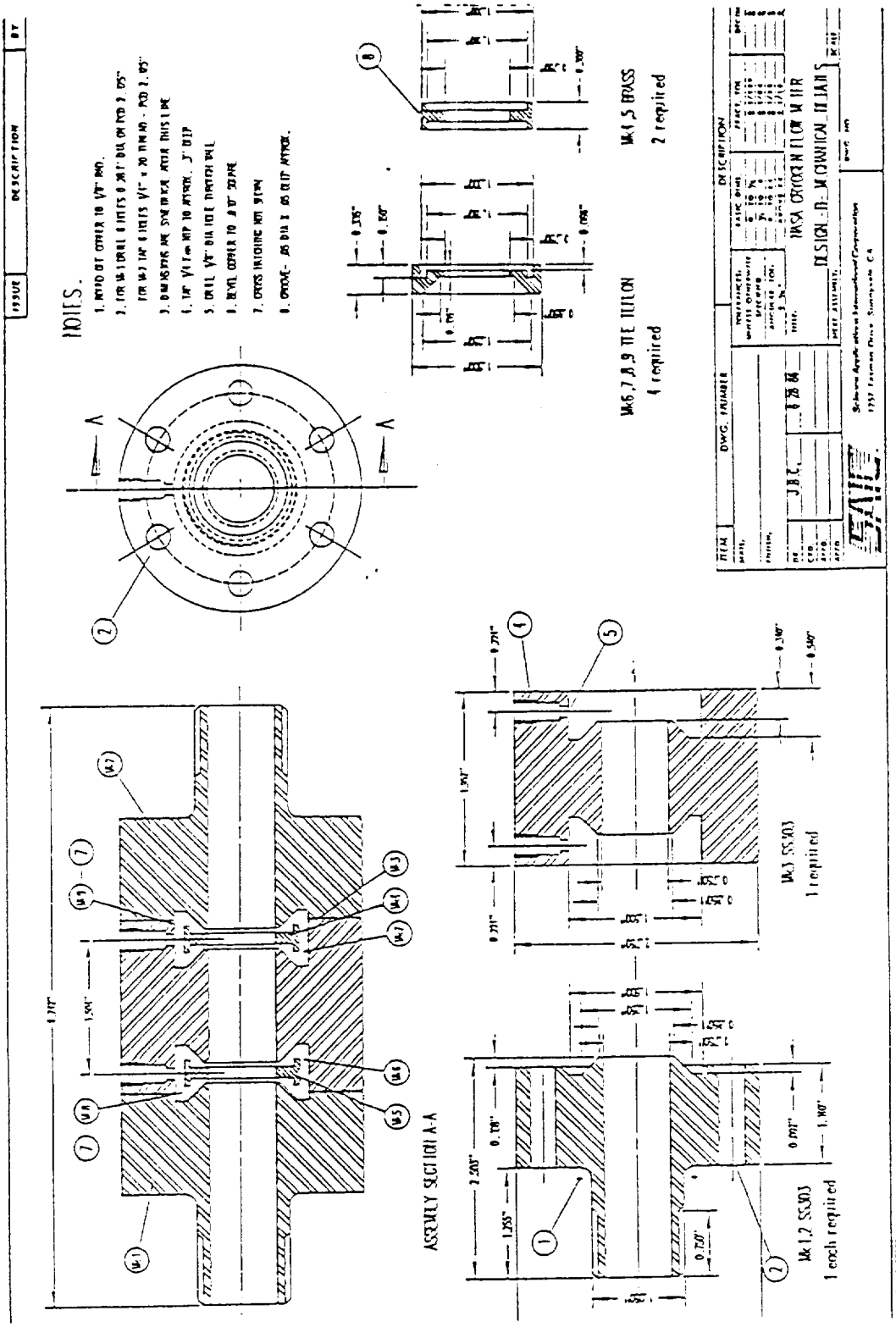

Figure 4.2

MECHANICAL DETAILS OF THE SPOOL PIECE DESIGN-B

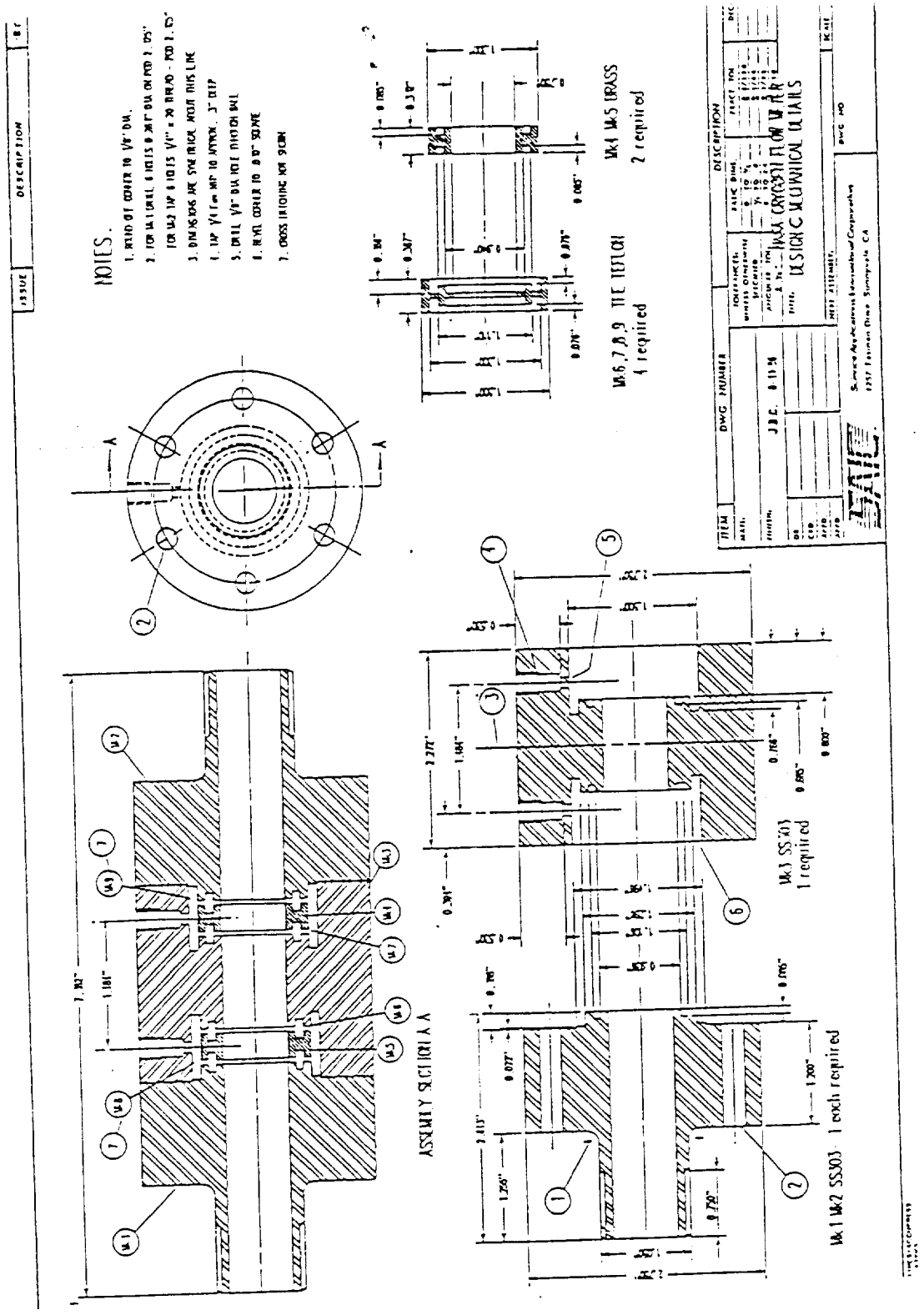

Figure 4.3

MECHANICAL DETAILS OF THE SPOOL PIECE DESIGN-C

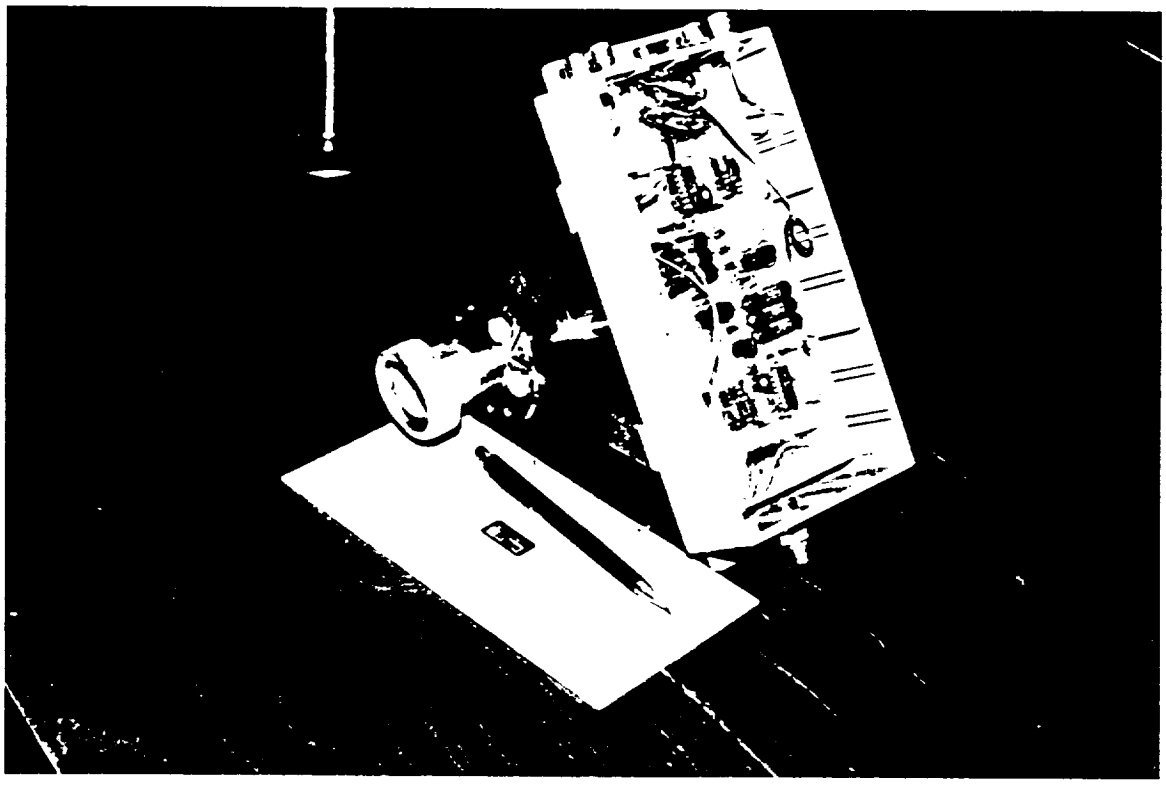

PLATE 4.1

DESIGN-C SPOOL PIECE WITH PREAMPLIFIER

4.2 Electrode and Insulator Design

The three spool piece designs have different electrode geometries. Designs A and B have the same electrode axial length of 3.35 mm but have different electrode axial separation. This provides a comparison between electrode separation of approximately one (design-A) and two (design-B) pipe diameters.

Design-C has a longer electrode axial length of 7.925 mm but the same electrode spacing as design-B. Hence comparison between designs-B and C provide a test of the effects of electrode axial length. All designs have the same teflon gap (1.27 mm) between the electrode and the pipe wall in the axial direction. The ideal electrode geometry would provide:

(a) wide bandwidth frequency response.
(b) low capacitance and high resistance to ground (spool piece body).
(c) small spatial sensitivity in the axial direction.
(d) equally sensitive to all areas of the pipe cross section or most sensitive to the region with the average velocity profile.
(e) good sensitivity to produce a large signal.
(f) facilitate a good seal.

Some of these requirements are conflicting and compromises must be reached. A short electrode supports (a) and (c) but may not support (d) and (e). Requirement (b) for low capacitance requires a small electrode surface area or a large gap between the electrode and the spool piece body. Large capacitance would conflict with requirements of (a), (c) and (f) but support requirements of (a) and (e) (a is conflicting because of large spacial coverage but supported because of low capacitance.). The electrode gap is important because of end effects which can only be predicted through numerical modeling which is beyond the scope of this work. These characteristics may have the greatest effects upon spacial sensitivity and signal strength. The electrode gap was selected primarily because of the thermal expansion and elastic limits of teflon. Careful consideration of these properties are required for a reliable seal.

The shape of the electrode and teflon seals is contoured to take advantage of radial shrinkage to provide sealing compression. The elastic limits of teflon are such that the elastic compression possible is only slightly greater that the contraction during cooling. Thus axial forces alone cannot provide an adequate seal.

Two seal designs were used. For designs A and B the teflon was beveled which enhances the axial forces during radial contraction. Design-C with a longer electrode has a simple profile that relies on the radial compression on the circumferential surfaces for sealing forces. The circumferential groove in the electrode assisted assembly and provided a void for compression of the teflon.

4.3 Electrode Connecting Wires

Consideration was given to the electrode connection wire to minimize capacitance to ground and the minimize vibration induced noise. Connection was made by 0.5 mm multistrand copper wire insulated with teflon. A schematic is shown in Figure 4.4. The wire was soldered into a hole in the circumference of the electrode. It then passed between the two halves of the teflon seal and through the electrode feed-through hole. This hole was also made a relatively large diameter to reduce the capacitance of the wire to ground.

The wire was supported in the shielding nipple that connects the spool piece with the preamplifier enclosure. The connecting wire was passed through a 1.5 mm diameter teflon tube to provide rigidity. Paper insulation was then packed around the teflon tube to fill the gap in the stainless steel nipple (6 mm internal diameter). This helped to dampen vibration and contain any moisture that may condense.

The connection wires then passed through holes in the preamplifier circuit board and were soldered to the component side. Some slack was left to facilitate reassembly and to ensure that there was no tension in the wire that would cause resonant vibration.

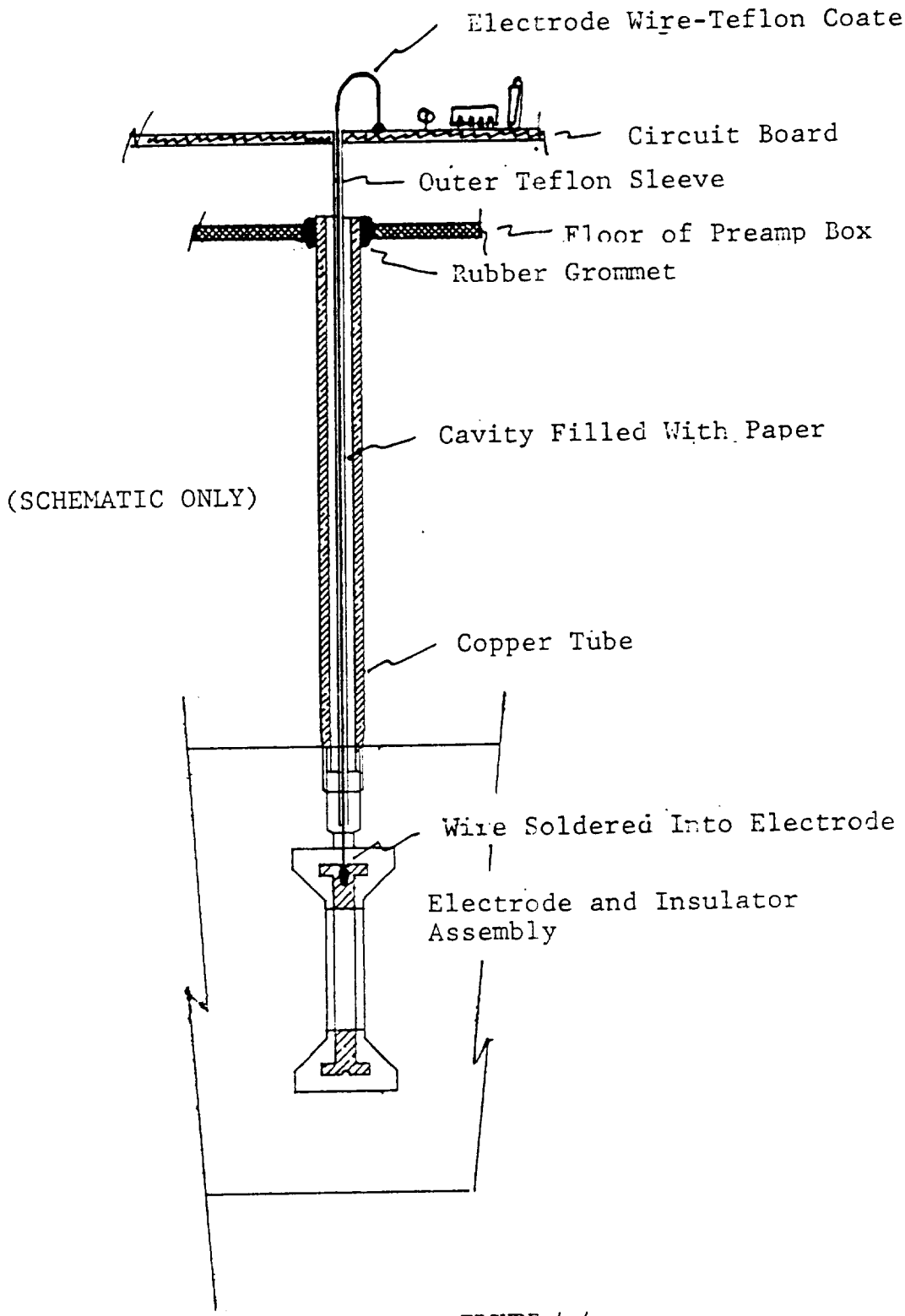

FIGURE 4.4

SCHEMATIC OF HOW THE ELECTRODE-PREAMPLIFIER CONNECTION IS MADE

5.0 ELECTRONICS DESIGN

5.1 Overview

The electronics for the TEFM consists of three functional units: 1. preamplifier, 2. signal conditioner, and 3. correlator. Signals from the electrodes are amplified by the high input impedance amplifier and transmitted to the signal conditioner. The signal conditioner filters the signals and converts them to binary or zero-crossing signals for input to the correlator. The correlator determines the cross correlation function between the two input channels and tracks the time delay associated with the peak in the correlation function. This time delay is inverted and output as a voltage signal proportional to velocity.

5.2 Preamplifier

Figure 5.1 shows a circuit of the preamplifier. The input stage is a high impedance (10^{12}ohms) buffer amplifier (LM210) used to prevent loading of the electrode signals. This impedance is of the same order as the resistivity of liquid nitrogen. A capacitor (C1) is used to couple the electrode signal to prevent dc offsets in subsequent stages. Such offsets arise from streaming potentials detected by the electrodes. Minor offsets (especially asymmetrical) would hamper operation of the zero-crossing detectors and prevent or at least bias the cross correlations.

Provision is made to short out this coupling capacitor and measure the streaming potential at the output of the high impedance buffer. Also various load resistors can be connected at the buffer input to reduce the input impedance. This facility is useful if the signals are large and/or have a lower source impedance. For normal operation high impedance, ac coupling is required in this application.

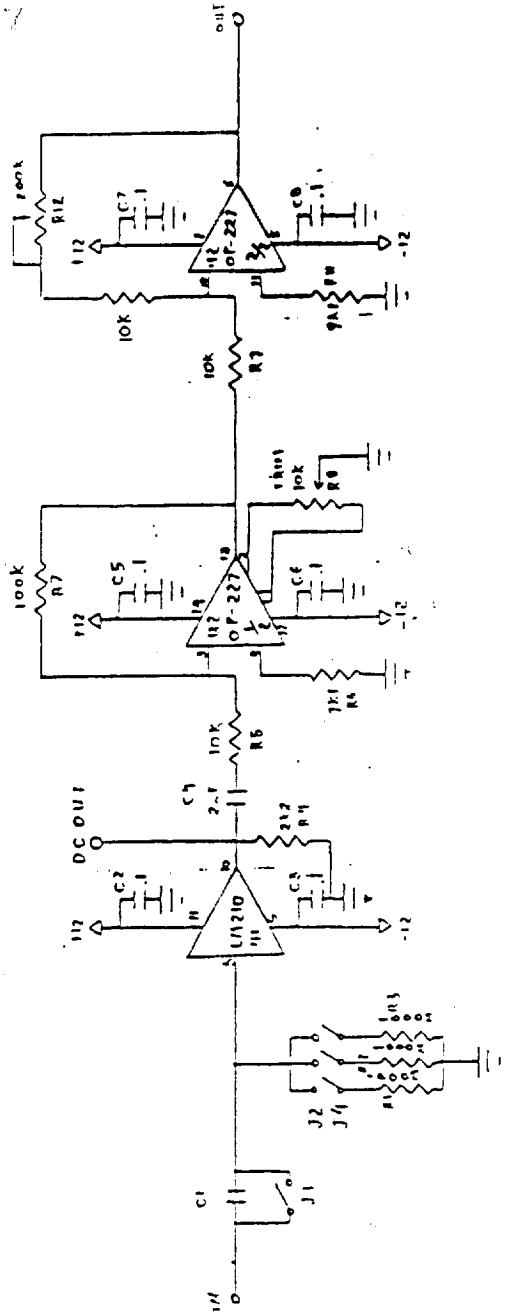

Figure 5.1

CIRCUIT SCHEMATIC OF THE PREAMPLIFIER

The gain stage of the preamplifier consists of two operational amplifiers (OP-227) providing an overall variable gain between 10 and 200. The frequency response provides a bandpass between approximately 2 and 3000 Hz. Since the triboelectric signal displays a 1/f (approximately) frequency spectrum most of the power lies in the lower frequency components (see 7.1.1). In theory there is a lower cut-off frequency below which both electrodes would lie essentially within the same charge packet. This would broaden the correlation peak and introduce auto correlation. The lower frequency depends on the flow rate and the electrode spacing. This was accounted for in the preamplifier by using the input capacitor but such fine tuning was not made in the subsequent circuits.

The circuits are produced on fiberglass printed circuit boards with the same layout for each channel (electrode). Both channels share the same power supply. The board is mounted in a die cast enclosure which is mounted to the spool piece as described in Section 4. Outputs from the buffer and gain stages are furnished through BNC connectors. Power is connected via a 9 pin "D" connector.

5.3 Signal Conditioner

The signal conditioner filters the triboelectric signals and converts them to a binary form. That is, if the signal is positive then the conditioner output is at logic 1 or in this case a high voltage. If the signal is negative then the output is logic zero or zero volts.

The circuit schematic is shown in Figure 5.2. It was adapted from another flow meter and contains features that were not required for this contract. The circuit shown can accommodate two flow meters and is mounted in a single width NIM electronics module.

The input active filter stage is built around a single operational amplifier (LM301) and has a bandpass response shown by Figure 5.3. This response function was shown to reduce the width of the cross correlation peak for freon flow thus producing improved time resolution. This is most likely due

ORIGINAL PAGE IS
OF POOR QUALITY

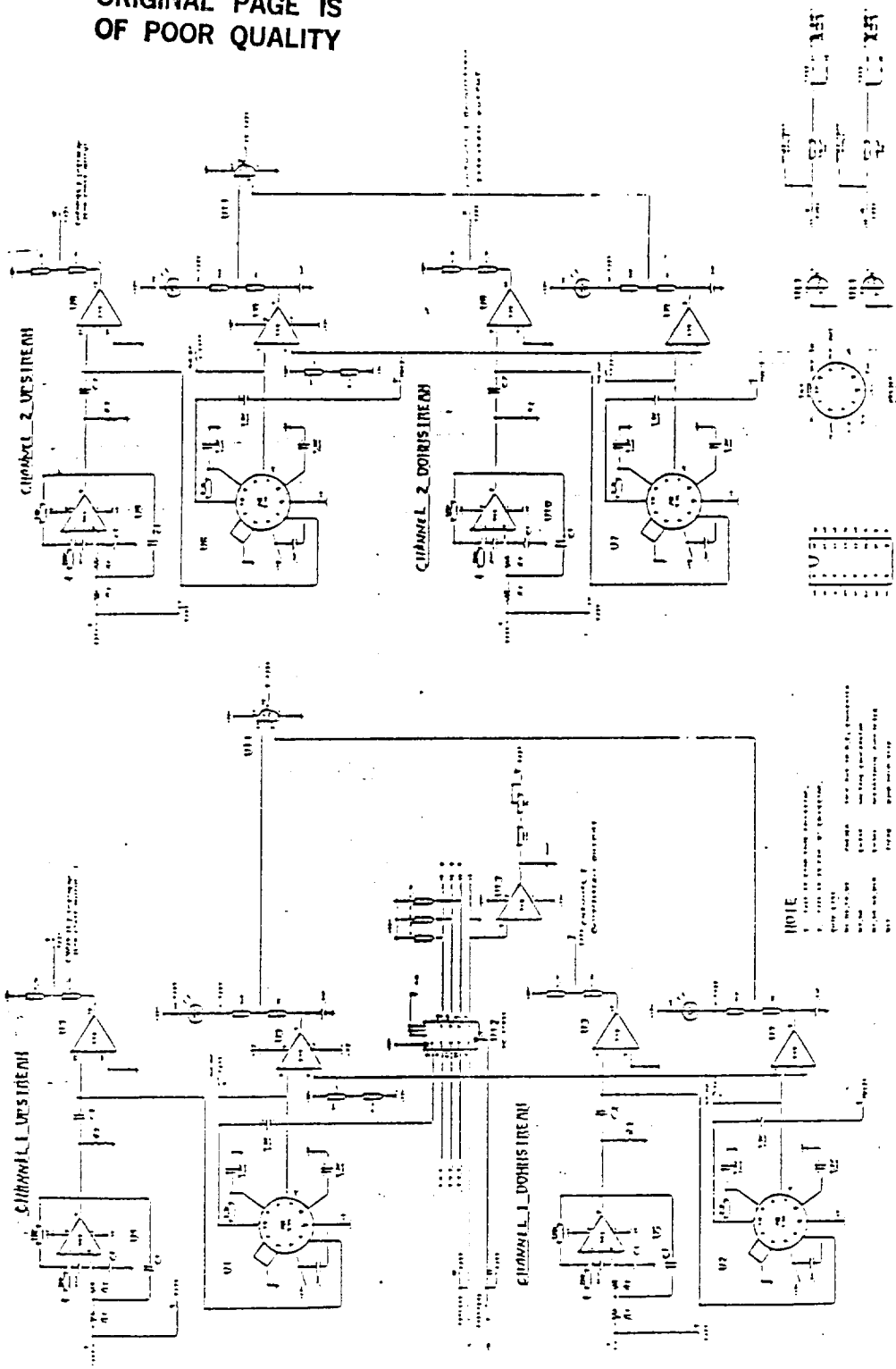

Figure 5.2

CIRCUIT SCHEMATIC OF THE SIGNAL CONDITIONER MODULE

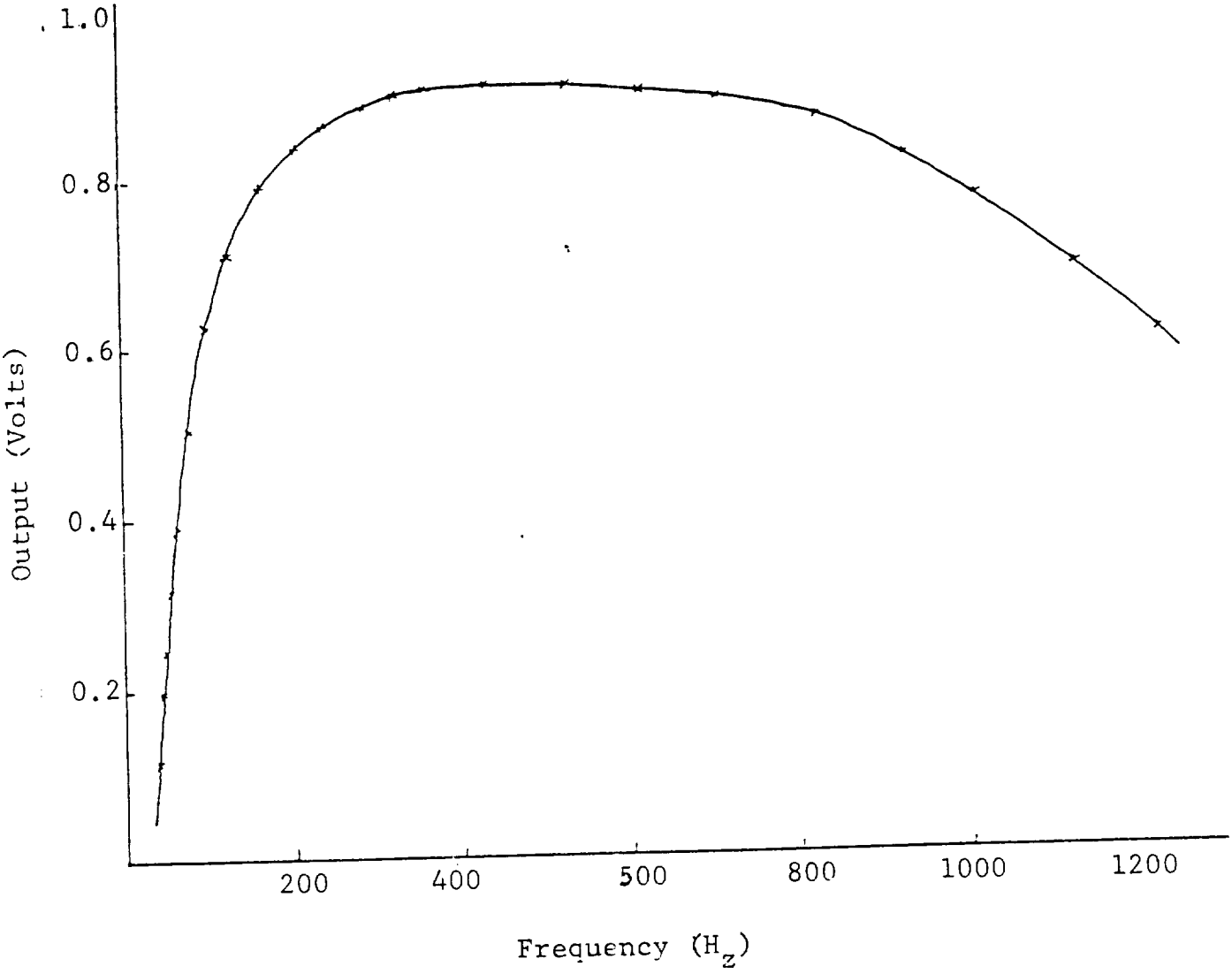

Figure 5.3

FREQUENCY RESPONSE OF INPUT STAGE FOR THE SIGNAL CONDITIONER MODULE

to a "prewhitening" effect by attenuating the lower frequencies which tends to even out the frequency distribution of the signal. Negligible signal from single phase flow existed above 1 KHz, at the lab flow rates.

Following the filter stage the signal branches to a comparator (LM339) for binary conversion and an rms level converter (AD536). The latter provides a dc voltage equal to the rms signal strength. The signal strength is available at a front panel meter by switch selection. Other features provided for the original application will not be described.

5.4 Cross Correlation

The correlator circuit was developed and designed from another application, however most of its features have been directly applicable to this contract. The circuit is completely hardware based and occupies a single circuit board mounted into a single width NIM electronics module.

The following is an overview of the important features of the cross correlation function. Table 5.1 summarizes the performance character-istics of the cross correlator. Briefly, the correlator accepts a binary conditioned form of the analogue triboelectric signals from each electrode. That is, the correlator input voltage signal is zero or 15V depending on whether the analogue signal is either negative or positive respectively. The upstream signal is sampled in 64 increments of time and stored. For the next 256 time increments, the downstream signal is sampled (64 time increments) and digitally compared with the stored upstream signal to perform the cross correlation. The cross correlation is done by a TRW correlator chip which outputs a 7 bit number representing the degree of correlation (converted to 8 bits for compatibility). At each of the 256 time delays this number is accumulated to produce the cross correlation function. The time delay corresponding to the maximum degree of correlation is the fluid transit time between the two electrodes. The circuit performs many other functions necessary for operation. The features essential for the TEFM are discussed below.

TABLE 5.1

Specifications And Features Of Prototype Cross Correlator.

Board Size	:	7 5/16 by 9 inches (187 x 229 mm)
Board Area Used	:	6 by 9 inches (153 x 229 mm)
Power Consumption	:	450 mA at 15 V
Voltage Range	:	12 to 16 V single supply
Inputs	:	Upstream Downstream (TTL), (one or two bits optional resolution) Bad Data flag (TTL)
Outputs	:	Lag of Correlation Peak (9 bit) Current Peak Correlation (Analog 0-10 V) X axis lag value (Analog 0-5 V in 256 lag mode) (Analog 0-10 V in 512 lag mode) Y axis correlation value (Analog 0-10 V) Velocity (Analog 1-10 V, with 1 volt representing maximum lag time)
Lag Resolution	:	256 or 512 points
Full Scale Lag Time	:	0.5 mS to 9.9 seconds
Sample Rate	:	512 KHz down to 52 Hz
Exponential Smooth T.C.	:	16 to 256 time Full Scale Lag times
Analog Smooth T.C.	:	Selected by an optional capacitor
Correlogram Output	:	Continuously updated and exponentially smoothed with time constants from 16 to 256 times full scale lag time
Fraction of Sampled Data Used	:	All Downstream 25% of Upstream (normal mode, 256 lags)
Resolution	:	2 bit Signal Inputs 7 bit Instantaneous Correlation 8 bit correlation (Y output) 8 bit current peak correlation 9 bit Lag Time (X output) 9 bit Data Outputs 12 bit Internal Math Calculations

Common mode rejection is important to eliminate effects of vibration and other noise that appears on the signals from both electrodes. This type of noise should be significant in the SSME. Such signals produce an auto correlation function that is added to the cross correlation function required for the measurement. This can bias the true correlation peak location and provide an erroneous reading. The value of common mode rejection has been demonstrated and is expected to be even more important in the SSME application because of the significant vibration and acoustical noise generated.

Another important feature of the correlator circuit is its ability to carry out a two-bit correlation. This allows for great precision or a faster response time. Work by Piersol and Bendat (reference) and others has shown the validity of using polarity converted signal. However, a longer sample is required to achieve the same precision as an analogue correlation as described in Section 3. Increasing the resolution to a two-bit conversion improves the precision. The addition of added bits of resolution further improves precision but with diminishing returns for the extra complication. The two-bit correlation can be achieved by a small add-on circuit, but still uses the single one-bit correlator. The two-bit option was not used in this work.

Smoothing of the cross correlation function is done at several stages in the correlation process. This allows for an optimal trade off between response time and precision while providing a continuous output of flow speed. Because the technique is based on a statistical process, data must be collected over a period of time and then "averaged" to produce a result.

Data collection is the accumulation of the cross correlation time function. The correlation is determined simultaneously at each incremental time delay from "zero" to the maximum time delay. A second correlation then begins immediately. Successive correlation functions are combined using the exponential smoothing technique which provides exponentially more weighing for the most recent data. The exponential time constant is adjustable in terms of the number of sweeps over which the data is smoothed. Exponential

smoothing is used commonly in process control to provide a smooth, yet rapid, response.

A further smoothing state is provided by the median time delay peak follower. After accumulating the correlation function, the time delay corresponding to the most correlation is determined. For high speed operation, a short exponential time constant is used, however this presents the likelihood of false peaks arising from noise at any other time delay. Such noise can also exist where the correlation peak is relatively weak and the false peaks can represent flow rates drastically different from the real rate. If the peaks were simply identified as the time delay with maximum correlation without smoothing, a very noisy flow signal may result.

Therefore, a median peak follower is used. The peak position is tracked by a pointer which is incremented by one time delay increment each sweep through the time span provided a peak is detected at a longer time delay. The reverse is true if a peak at shorter time delay is detected. Should the new peak be false then the error is much smaller than if the average (exponential or otherwise) peak location were used. This technique is statistically much more immune to noise than conventional techniques. For good data which is highly correlated, the facility can be disabled to revert to instantaneous peak following.

The flow signal output from the correlator is a 0-10V DC signal proportional to flow rate. The inversion of time delay is done internally by a novel use of a digital to analog converter chip. Smoothing of this output is done by a simple RC network representing a third smoothing stage. A digital output is available for the time delay signal (9 bit).

Other outputs include signals for x and y oscilloscope inputs to display the correlation function with time delay, and the value of the correlation function peak. The latter is a measure of the quality of the cross correlation.

6.0 EXPERIMENTAL SET-UP AND TEST PROCEDURE

Three basic arrangements were used for testing cryogenic and non-cryogenic fluids. Non-cryogenic fluids such as freon, water and transformer oil were used in a laboratory set up to develop the spool piece and preamplifier designs. A separate laboratory flow loop was used for liquid nitrogen flow testing and a portable version of this was used for test at a liquid nitrogen supply depot.

6.1 Non-Cryogenic Flow Loop

Figure 6.1 shows a schematic representation of the flow loop used for non-cryogenic fluids. A magnetic coupled drive, variable speed rotary pump was used to circulate fluid from a tank, through the test piece and back to the tank. Flow rates up to 30 liters per minute (l/min.) of liquid freon were obtained.

Readings from the triboelectric flow meter were compared with a reference flow meter installed downstream in the loop. This was a 3/4" diameter turbine flow meter with a linearization circuit capable of providing 0.1% accuracy. The turbine meter was calibrated by the manufacturer using water. All piping in the set up was 3/4" schedule copper tube.

6.2 Cryogenic Fluid Test Set-Up

6.2.1 Laboratory Set-up

Liquid nitrogen was used in the laboratory for cryogenic testing of the TEFM. Figure 6.2 shows a schematic of the set-up used. Liquid nitrogen was passed from a standard (high pressure) dewar (196 liters) through the TEFM spool piece and the turbine flow meter to an empty dewar. Dry nitrogen gas was used, where required, to pressurize the "source" dewar to obtain higher flow rates. The maximum practical flow rate of approximately 40 l/min provided for approximately 5 minutes of continuous flow.

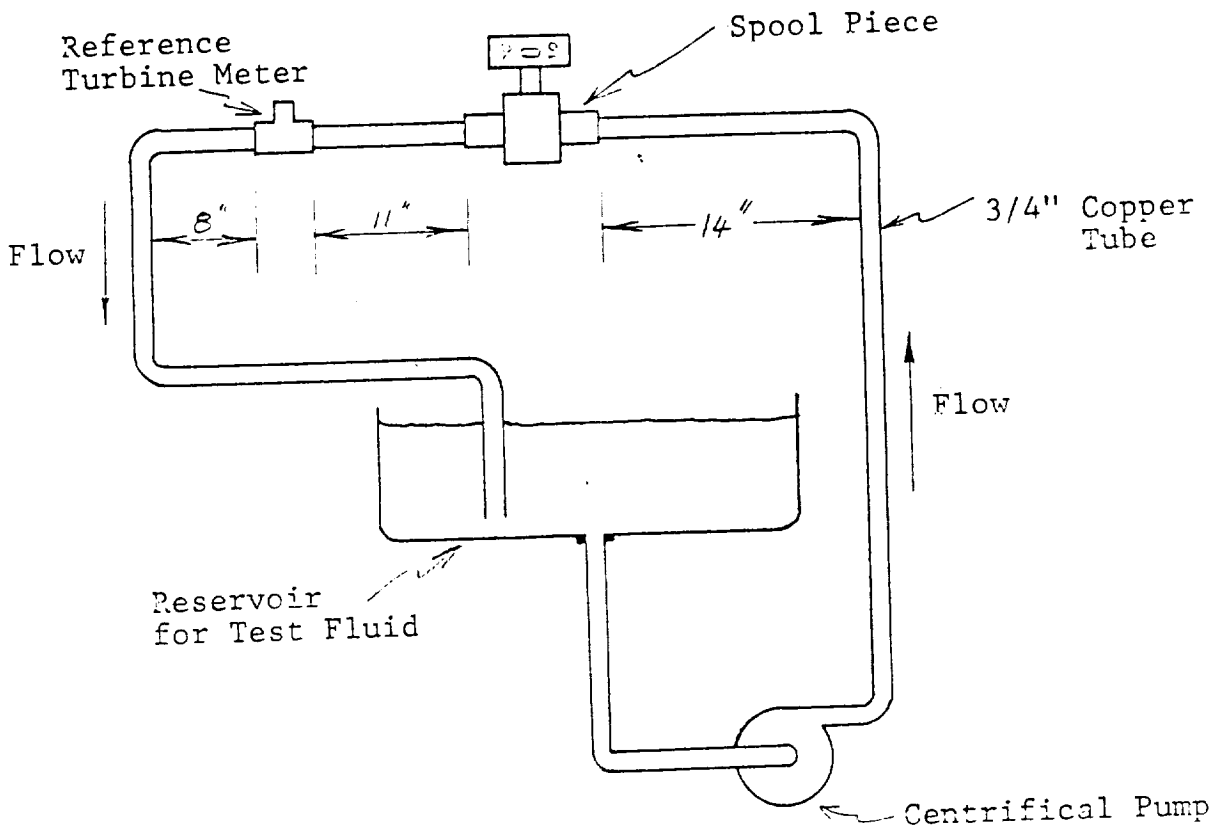

Figure 6.1

FLOW LOOP FOR TESTING OF SPOOL PIECES WITH
FREON, WATER AND TRANSFORMER OIL

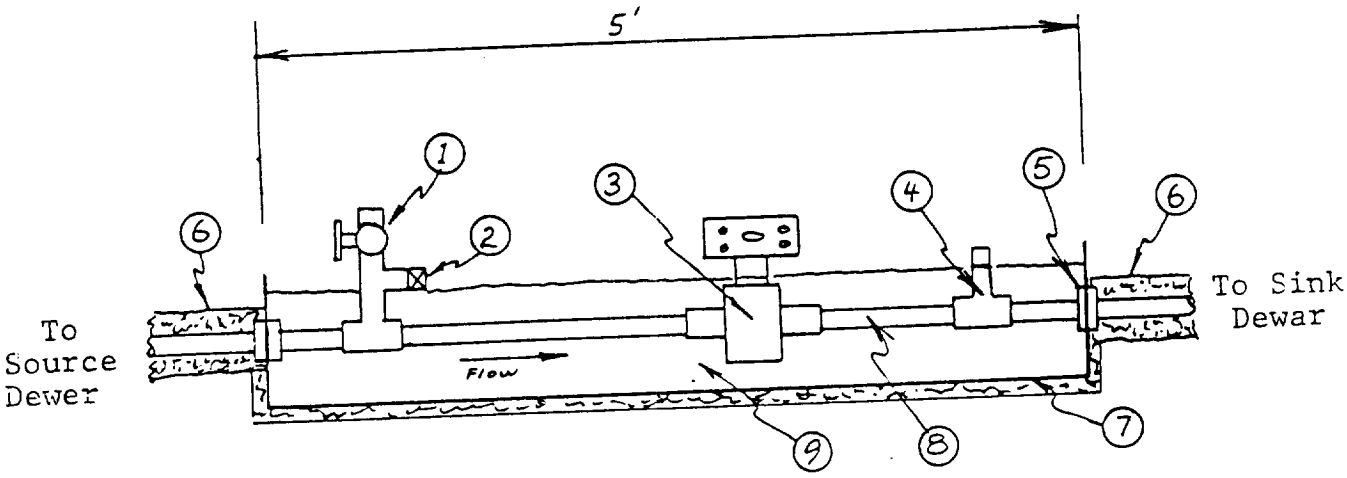

1. Vent valve.
2. Pressure relief valve.
3. Test spool piece with preamplifier (heating & N_2 purge not shown).
4. Turbine flow meter.
5. Bulk head gland and teflon seal - tightened after cool down to allow for thermal expansion.
6. Rubber thermal insulation around tube to dewars (approx. 8" long).
7. Metal trough (6" dia. tube) filled with LN_2 and insulated.
8. Schedule 80 copper tube 3/4" diameter.
9. LN_2 bath.

Note: -The trough was covered with a lid (not shown).
-Dewars and N_2 gas for propellant are not shown.

Figure 6.2

LABORATORY TEST SET-UP FOR LIQUID NITROGEN

To minimize the risk of boiling, the piping between the dewars (approximately 2m), including the flow meters were immersed in a bath of liquid nitrogen. The preamplifier which was mounted to the spool piece was purged with nitrogen gas and heated to prevent moisture condensation over the high impedance circuit. The short (0.2m) dewar connecting tubes were wrapped in 25mm rubber insulation. The flow rate was regulated using the "sink" dewar valve with the source dewar valve fully open. This kept the test section under pressure and helped to prevent boiling and cavitation.

Various pressure release valves and regulators were installed for safety. All tubing was 3/4" schedule 40 copper which was tested with each spool piece to approximately 1.3 MPa (200 PSI) at cryogenic temperatures. Only a 3/8" diameter output tube was available from the dewars and reducers were used to couple with the 3/4" tubing.

Plate 6.1 shows a photograph of the laboratory test set-up.

6.2.2 Depot Test Set-up

Tests were also made at a liquid nitrogen supply depot to take advantage of the large supply of sub cooled liquid nitrogen. To provide pre-cooling, the spool piece section was mounted in a styrofoam cooler and filled with liquid nitrogen. This provided a portable equivalent of the laboratory set up. The turbine flow meter section was insulated with 25mm thick foam rubber.

This arrangement was mounted as close as possible to the outlet valve of a large supply tank as shown in Plate 6.2. Liquid was allowed to flow through the set-up to one or two standard dewars (in parallel). Throttling was controlled at the dewar inlet valve to maintain pressure in the spool piece. Flow rates in excess of 55 l/min were possible depending on the level within the storage tank. This is only 2% of SSME flow rate.

Preamplifier heating and nitrogen purging were also supplied as for the laboratory set-up.

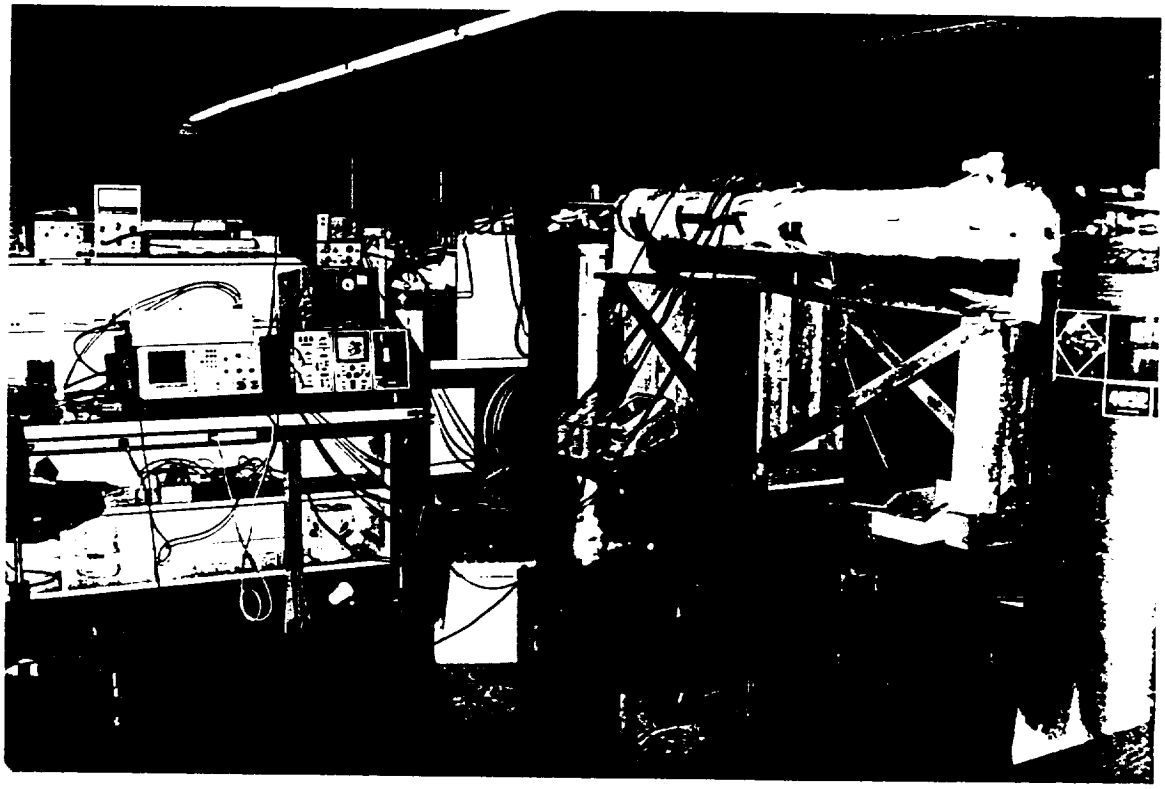

PLATE 6.1

LABORATORY SET-UP FOR TESTING LIQUID NITROGEN FLOW

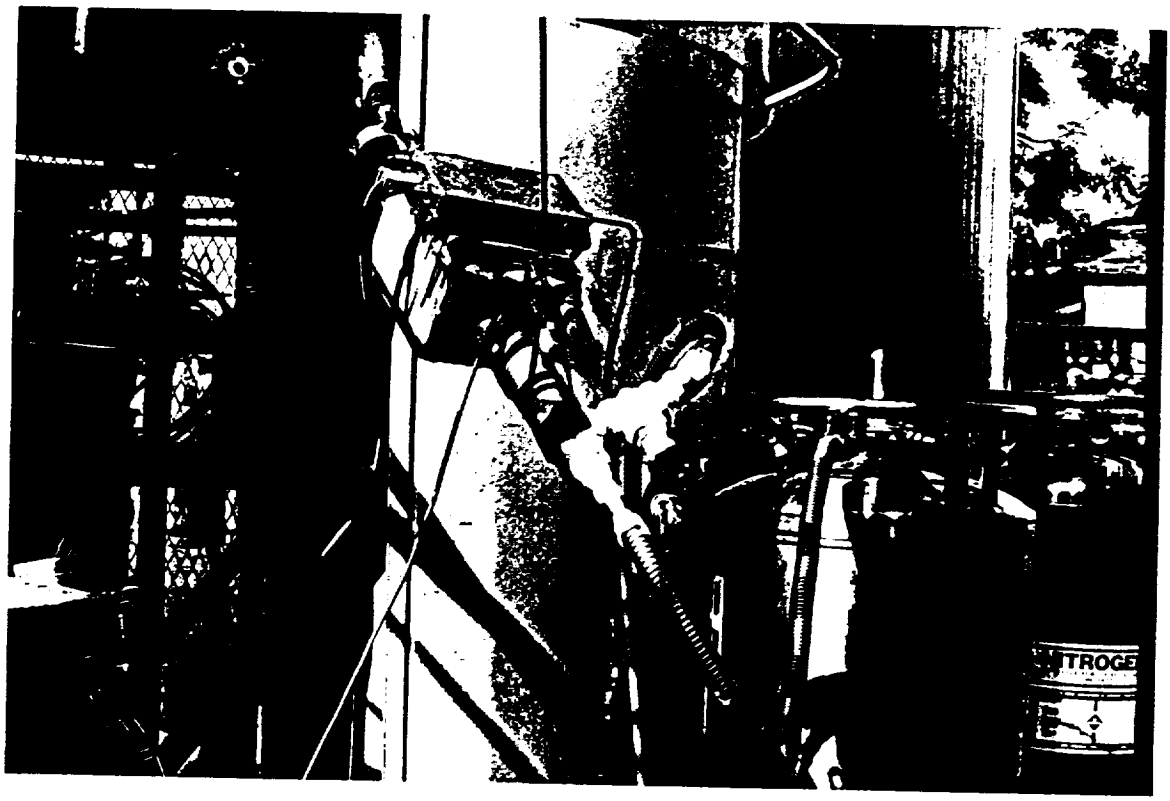

PLATE 6.2

LIQUID NITROGEN DEPOT TEST ARRANGEMENT

Tests were also made with an extended length of pipe between the spool piece and the supply tank to allow a greater path length for charge accumulation. This extension consisted of a 3/4" galvanized steel pipe approximately 1 meter long. For precooling it was mounted coaxially within a 3" pipe section to provide a jacket that was filled with liquid nitrogen. Fibre glass insulation was used to minimize the liquid nitrogen burn-off.

6.3 Data Recording and Test Electronics

Figure 6.3 shows a schematic of the data recordings and test electronics. The TEFM electronics are described in Section 5. The following voltage outputs from this electronics were recorded using a desk-top data logger and computer with floppy disk storage:

- Velocity proportional output
- Peak correlation function (relative)
- Triboelectric noise signal strength (rms voltage)

The pulse signals from the turbine flow meter were processed by the linearizer and then input to a rate meter to provide a voltage signal proportional to flow rate. This signal was also input to the desk top data logger.

A storage oscilloscope, with floppy disk, was used to record the correlogram (cross correlation function) from the cross correlator. Other signals were also recorded in this way for analysis and plotting.

A spectrum analyzer was used to collect and plot the frequency spectrum of the triboelectric noise signals. Other standard test instruments such as a digital multimeter, megohm meter, and an electrometer were also used.

Data from the desk top computer was transferred to a personal computer for analysis using standard spread sheet software.

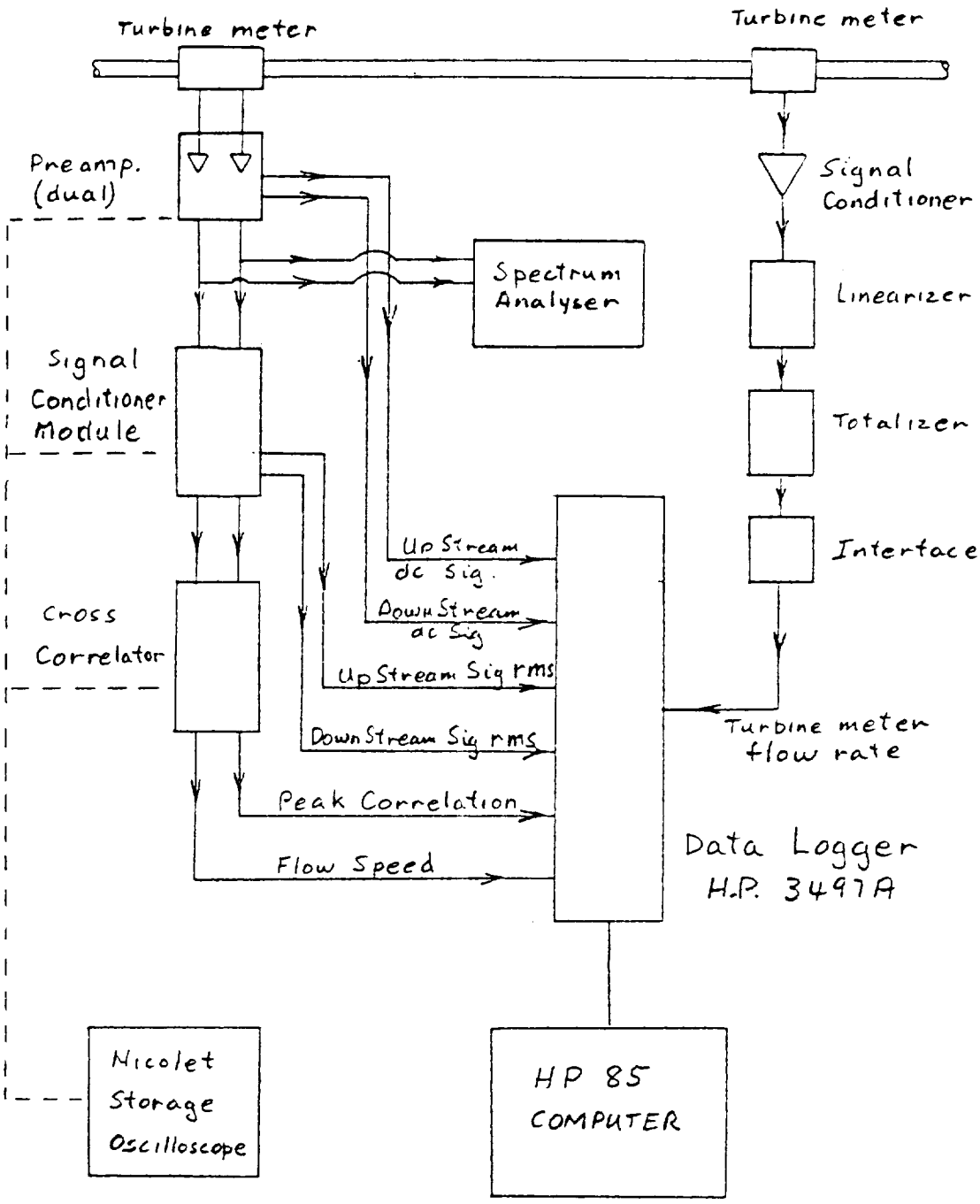

Figure 6.3

SCHEMATIC OF DATA RECORDING AND TEST ELECTRONICS

6.4 Test Procedures

The primary purpose of the test was to provide a comparison between the flow rates measured using the TEFM and the turbine flow meter. The most successful TEFM design is the one which yields the best measurement precision under similar experimental conditions.

6.4.1 Non-cryogenic Flow Tests

The raw data was recorded by adjusting the pump speed to maximum flow rate and then reducing it in incremental steps to the minimum practical flow rate. At each step data was recorded by the data logger at 2 second intervals. A minimum of 3 readings were made at each step comprising between 80 and 200 data points for each spool piece. Each data point consisted of: the outputs from the TEFM and turbine flow meter, the peak cross correlation function, and the triboelectric signal strength. The flow rate was allowed to stabilize for approximately 30 seconds before data was recorded.
The raw data were then transferred to a personal computer and the flow rates in engineering units were calculated and plotted. Least squared linear regression was applied between the TEFM and the turbine flow meter to make quantitative performance comparison.

The absence of bubbles within the flow loop was confirmed by installing a clear tube after the turbine meter. Deliberately induced bubbles were clearly seen through the tube but none were generated during the test period.

An indication of the effective "bandwidth" of the binary converted triboelectric signal was obtained by inputting the same signal (from one electrode) to both inputs of the cross correlator. This provided an autocorrelation function from which the average rate of zero - crossing could be determined. The implications of this are discussed in Section 3.

Auto correlation was performed at approximately 10 flow rates for each of the spool piece designs B and C. Design A and B differ only in electrode separation and have the same electrode frequency response.

The spectrum analyzer was used to record frequency spectra of the analog triboelectric signals directly from the preamplifier.

Test work was also carried out on early version of the TEFM. In particular the d.c. streaming potential was measured at various flow rates. The application of the TEFM to water and transformer oil was also confirmed. Smaller amounts of data were manually recorded for these tests since they did not require vigorous analysis. Also a visual reading rotameter was used as the reference meter in place of the turbine meter.

6.4.2 Cryogenic Flow Tests

Special procedures were followed before testing with liquid nitrogen. After assembly of the various flow loop components the system was pressure tested for leaks. Before precooling of the assembly, the valve on the sink dewar (empty) was cracked open to allow a small flow of gas through the flow meters and out of the vent valve. This ensured that the system was dry and that the turbine meter was operational. Filling of the precooling trough was begun while maintaining flow of gas through the system. Periodically the test section was pressurized during cool down to ensure the absents of leaks. Preamplifier purging and heating was also begun during cool down.

Following cool down, preamplifier operation was checked and the "source" dewar was pressurized with dry nitrogen gas. The test section vent and the sink dewar inlet valves were then closed. The source dewar valve was then opened to apply full pressure to the test section. The sink dewar vent and inlet valves were then opened as required to begin the tests. Data was then collected as described in Section 6.4.1. A similar procedure was followed at the liquid nitrogen depot. To obtain higher flow rates the LN_2 was vented to the atmosphere for approximately 30 seconds. All the data logging and test electronics were set up on site.

7.0 TEST RESULTS AND DISCUSSION

7.1 Non-cryogenic Tests

7.1.1 Triboelectric Noise Characteristics - Freon

The triboelectric flow noise from the ring electrodes ranges in amplitude from approximately 100 to 200 mV rms for flow rates between 10 and 20 l/m respectively. Figure 7.1 shows how the signal strength increases with flow rate. Since the preamplifier has an overall gain of 200, the true potential from the electrodes range between 1 and 2 mVrms over this range. Peak to peak voltages can be factor of 10 above these levels. This signal strength is more than adequate to drive the zero crossing detectors (comparators). The comparators are essentially independent of signal strength even if the gain of the two electrode amplifiers differ greatly. The preamplifier and signal conditioning circuits require that the signals do not saturate. This would produce artifacts that may bias the correlation.

Typical triboelectric signal frequency distributions are shown in Figure 7.2. The spectra are heavily distributed about the low frequencies below 100 Hz and fall off inversely with frequency (i.e. "1/f noise). As shown in Section 5.3 the signal conditioner filters ("whitens") this distribution slightly with a low frequency roll off at approximately 90 Hz. Therefore, the average rate of zero crossing is typically between 50 and 100 Hz. This spectral "whitening" effect was found to improve the cross correlation resolution by effectively increasing the binary signal bandwidth.

The effect of electrode length on the frequency response is evident from the auto correlation function of each signal (ref). Figure 7.3 shows a typical set of auto correlation functions for design-B. For a random, single bit digital signal the auto correlation function represents an exponential function in time and the decay constant is inversely proportional to the

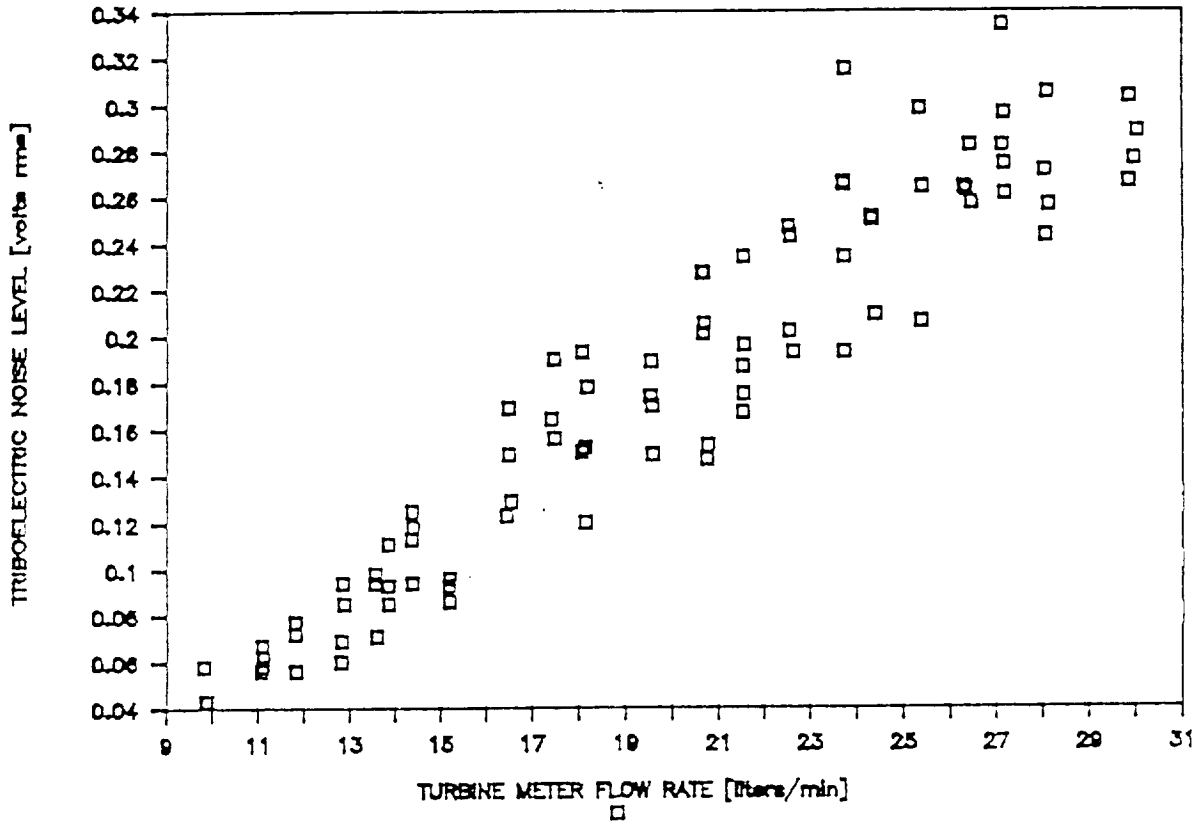

Figure 7.1

VARIATION OF TRIBOELECTRIC SIGNAL STRENGTH
(VOLTS-rms) WITH FREON FLOW RATE

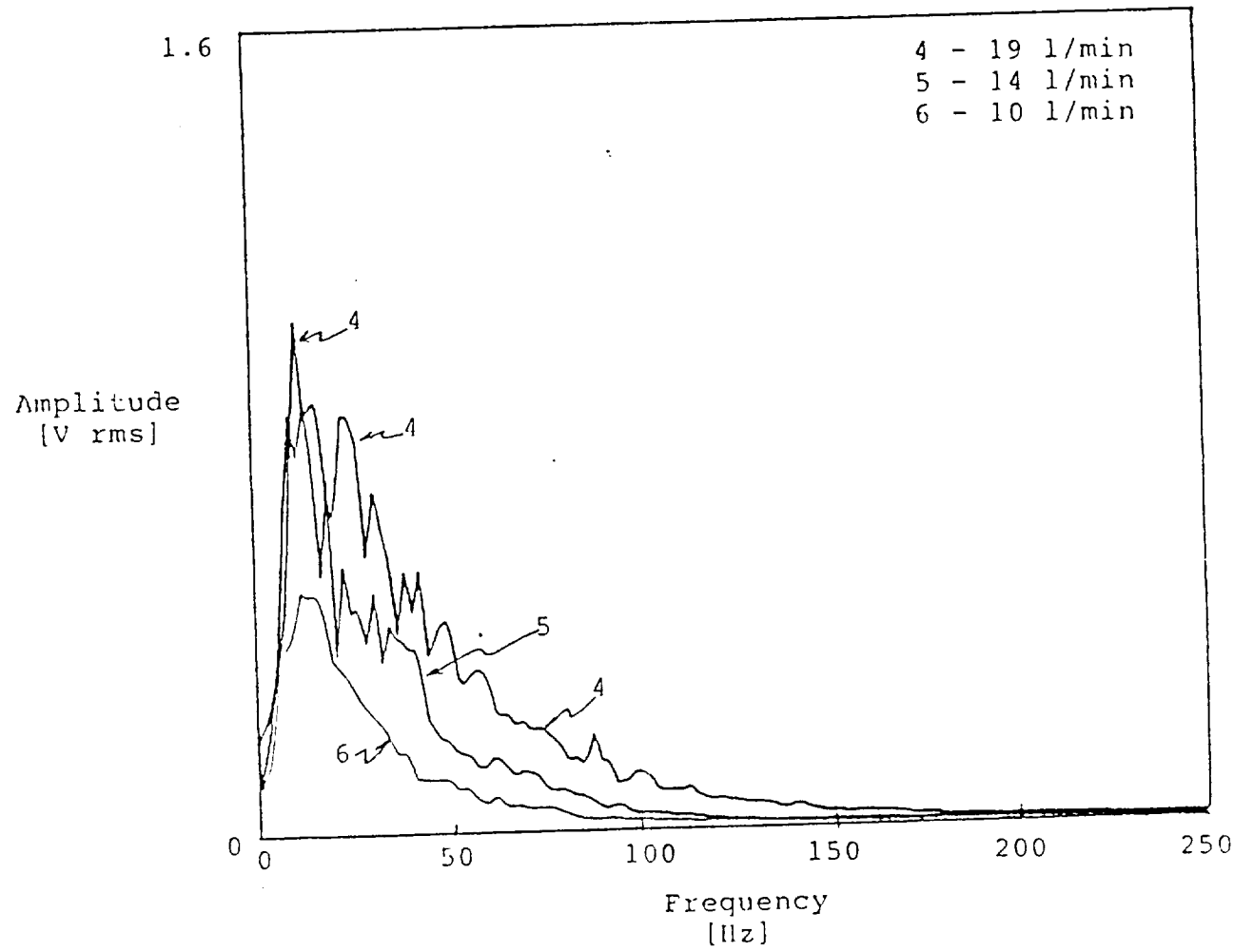

Figure 7.2

TYPICAL FREQUENCY DISTRIBUTION OF TRIBOELECTRIC NOISE FROM DESIGN-A ELECTRODES WITH FREON FLOW

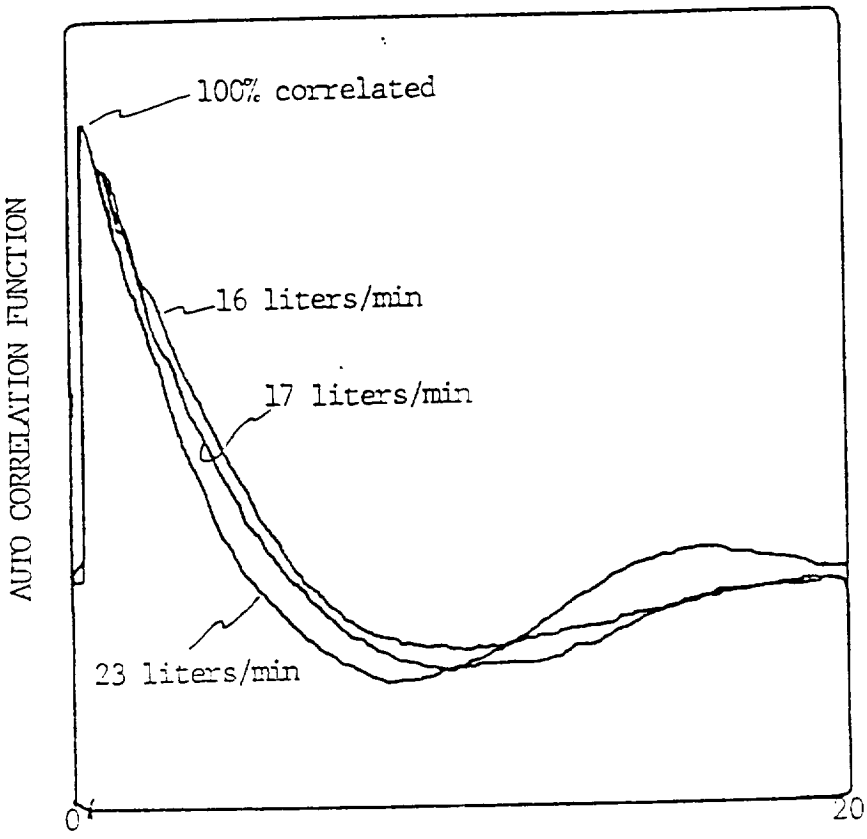

Figure 7.3

TYPICAL AUTO CORRELATION FUNCTIONS OF FREON GENERATED SIGNALS FROM DESIGN B

average zero crossing rate. By sampling and counting, it was found that the average zero crossing rate is equal to

$$\text{Rate} = 1/(4t')$$

where t' is the exponential decay constant. This rate was determined for designs B and C and the results are shown in Figure 7.4. As expected, the zero crossing rate increases with flow rate for both designs. For design-C at 20 l/m the rate is approximately 46 Hz compared with approximately 68 Hz for the shorter electrode of design B. This gives design-B a higher frequency response which should enhance the velocity precision of design B compared with design C. This expectation is confirmed in the next section.

7.1.2 Velocity Determination - Freon

Velocity determination using freon was highly successful for all spool piece designs. The cross-correlator determined the classically shaped cross-correlation function (correlogram) that behaved as expected with variation in flow rate. Figure 7.5 shows a typical set of correlograms for spool piece design-C at various flow rates. The location of the peak moves towards longer time delays as the flow rate is decreased. Also, the "width" of the peak increases with decreasing flow rate and will be considered subsequently.

Figures 7.6 to 7.8 show plots comparing the flow rate determined using the TEFM and the turbine flow meter for spool pieces A to C respectively. The turbine flow meter results are linear with the TEFM for each design. There is, however, a proportionality constant or gauge factor and a small offset to be applied to the TEFM readings to make them equal the turbine meter reading. The offset is most likely due to electronic offsets within the correlation circuit. The gauge factor results from effects of the velocity profile across the diameter of the tube. Since the TEFM's always read the same or higher flow rates, the electrode response is dominated by the fluid regions away from the tube wall.

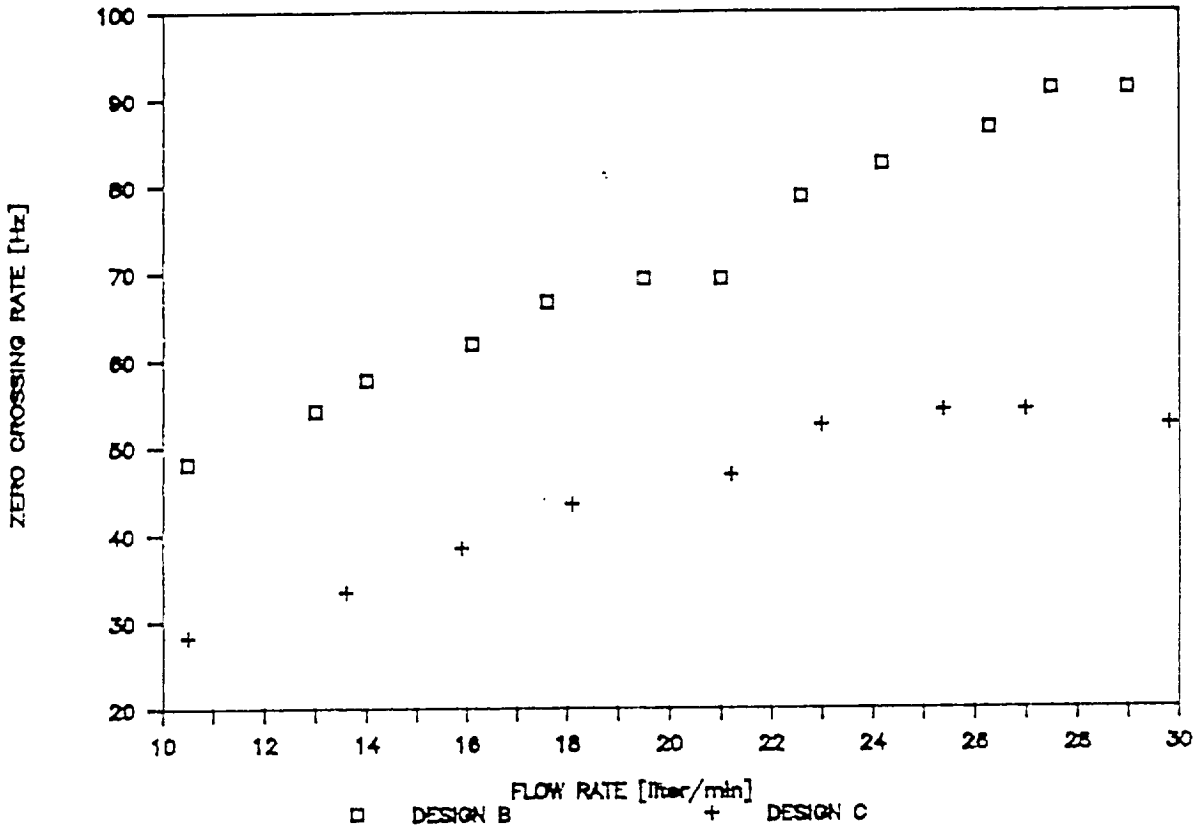

Figure 7.4

AVERAGE ZERO CROSSING RATE FOR TWO ELECTRODE LENGTHS - 3 AND 8mm FOR DESIGNS B AND C RESPECTIVELY

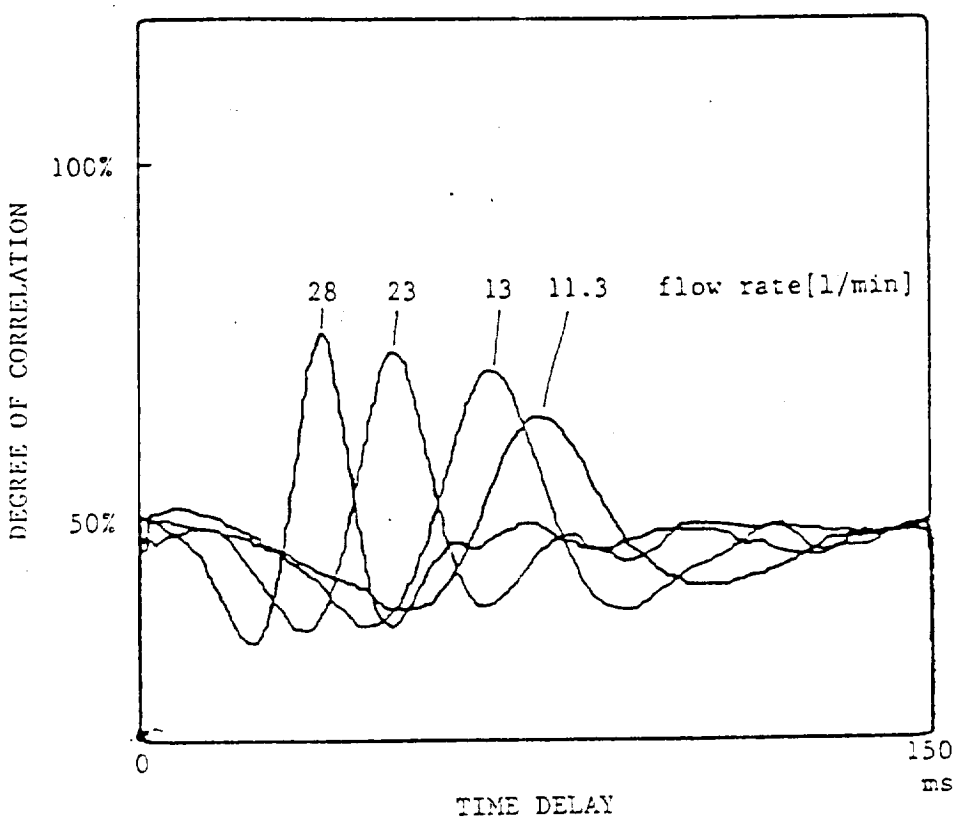

Figure 7.5

TYPICAL CROSS CORRELATION FUNCTIONS FOR SPOOL PIECE DESIGNS C AT VARIOUS FLOW RATES-FREON

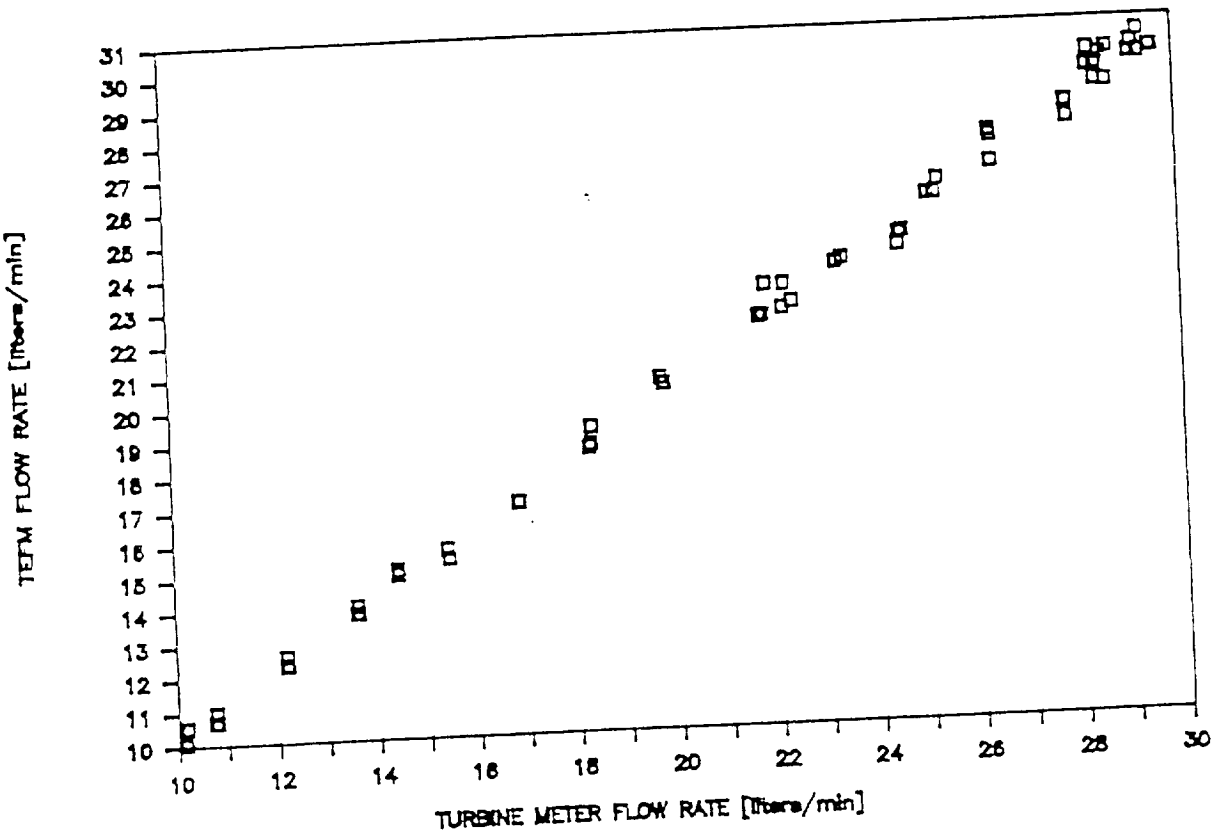

Figure 7.6

COMPARISON BETWEEN THE FLOW RATES DETERMINED BY THE TEFM-DESIGN A AND THE TURBINE FLOW METER. THE TRIBOELECTRIC SIGNAL STRENGTH IS ALSO SHOWN

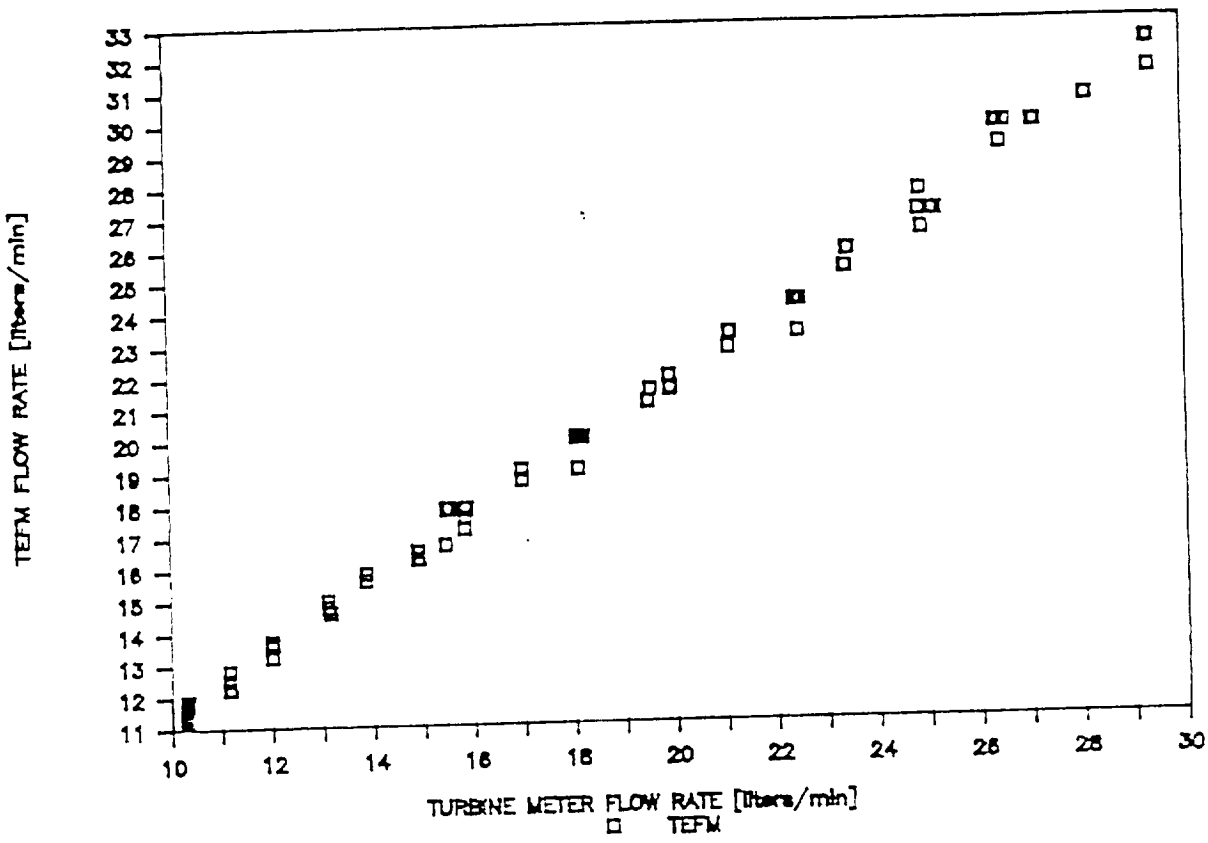

Figure 7.7

COMPARISON BETWEEN THE FLOW RATES DETERMINED BY THE TEFM-DESIGN B AND THE TURBINE FLOW METER. THE TRIBOELECTRIC SIGNAL STRENGTH IS ALSO SHOWN

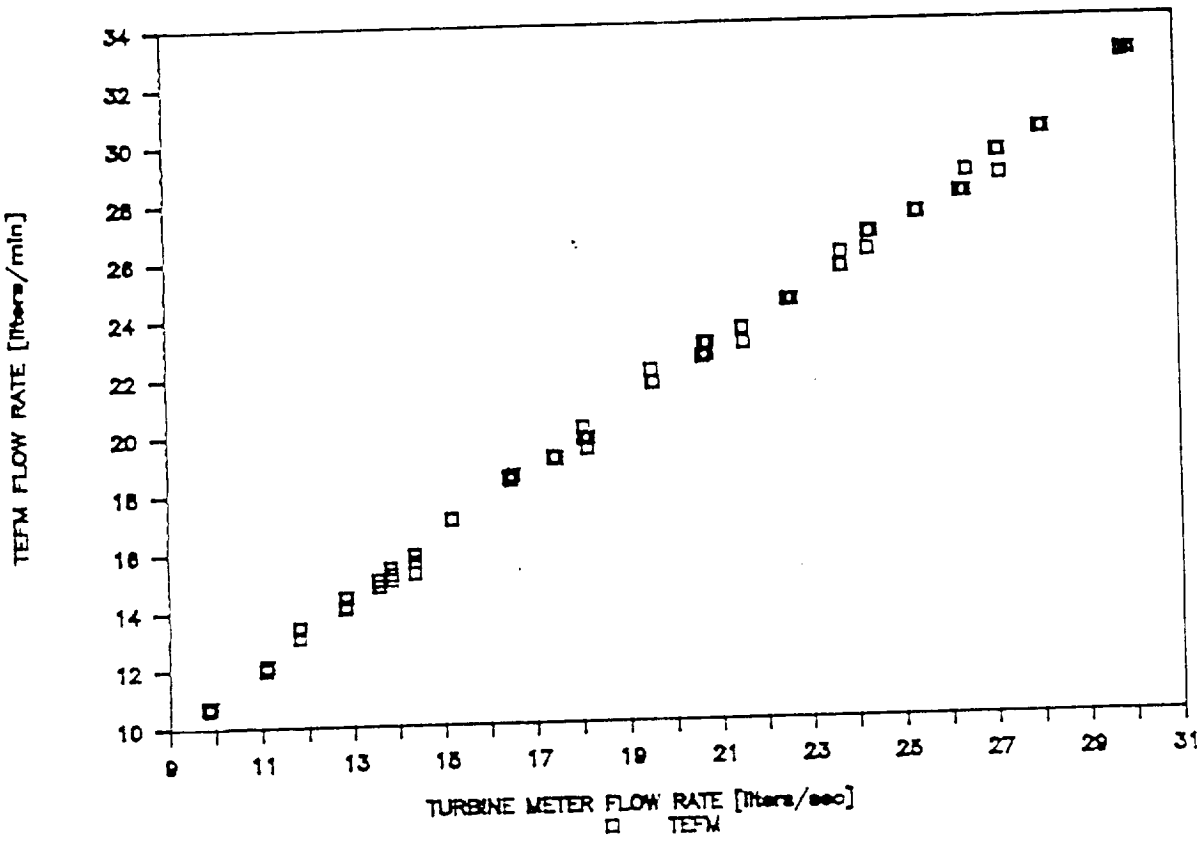

Figure 7.8

COMPARISON BETWEEN THE FLOW RATES DETERMINED BY TEFM-DESIGN C AND THE TURBINE FLOW METER. THE TRIBOELECTRIC SIGNAL IS ALSO SHOWN.

Table 7.1 summarizes the calibration results for each spool piece. Design A has a gauge factor almost equal to one (.97) and a small offset of 0.2 1/m. This result is very encouraging. It shows that, for design A, the total system (geometry and electronics) is reasonably well matched to respond to the average flow profile and is in effect an absolute flow meter. The results for designs B and C are interesting since the two designs have the same electrode separation and use the same correlator settings. Both designs have essentially the same gauge factor and offsets of approximately 0.93 and -0.5 1/m respectively. This demonstrates that the long and short electrodes have the same response to the flow velocity profile. The gauge factor less than one suggests that the slower moving regions near the pipe wall drop out of the correlation causing the response to be biased by the faster flowing regions towards the middle of the pipe.

TABLE 7.1

Performance and Calibration Results For Each Spool Piece Tested With Freon.

	Design A	B	C
Electrode spacing [mm]	19.355	38.202	37.694
Electrode length (axial) [mm]	3.353	3.353	7.925
Calibration constant (slope)	.965	0.9345	0.9399
Calibration constant (off set)	0.2161 .4589	-0.5182	-.4956
rms error of estimate	.3	0.4	0.3
Resolution of peak at 20LPM [%]	---	32	40
Average zero crossing rate	---	70	46

Each design shows very similar precision. Designs A, B, and C show precisions of 0.3, 0.4, 0.3 1/m, respectively. Design-A, has a shorter electrode separation allowing for a shorter correlation time span and hence a faster response. Since 128 correlator time spans were used for exponential smoothing for all the data, design-A had a smoothing time constant of 6.4 seconds compared with 20.2 seconds for designs-B and C. At real flow rates

in the SSME these time constants would reduce to less than 1 second. Design-B has the same electrode length as design-A but has a longer electrode spacing and gives a slightly poorer precision of 0.4 l/m. The significance of this small difference is not great. However, it fits the hypotheses presented in Section 4. The shorter electrode responds to smaller eddies resulting in a higher frequency response (Section 7.1.2). While this is expected to improve the resolution, the smaller eddies change relatively quickly. Hence, the two electrodes must be relatively close for the smaller eddies to correlate and improve the effective precision.

Accuracy is generally quoted as the difference between the device under test and standard or absolute device. Since the TEFM response is so linear, the accuracy after calibration is equal to the precision discussed above. If the response function were not linear, then a separate accuracy could be determined which would vary with flow rate. Thus, for these spool pieces, once the calibration equations have been determined (offset and gauge factor) the accuracy is within the precision of the determination.

In order to further discriminate among the designs, the velocity resolution of each design was determined. The resolution was taken as the "width" (in terms of velocity) of the cross-correlation peak at half its peak height (in terms of % of correlation). As shown in Table 7.1, the resolution for designs-B (32% at 20l/m) is better than for design-C (40% at 20l/m). As discussed, design C has a longer electrode and hence a lower frequency response and is expected to yield poorer resolution. Figure 7.9 shows the resolution for designs B and C plotted against flow rate. Here, the percentage resolution, in terms of the percentage of the velocity, increases with increasing flow rate. This result is unexpected and unexplained.

The height of the correlation peak is an indication of the degree of correlation. Since the TEFM requires only the location of the correlation peak, the peak height is important only in that it must remain higher than the "background" correlation function. Figure 7.10 shows the peak height as a function of flow rate for designs B and C. The peak height increases with increasing flow rate as expected. Design C shows a higher degree of

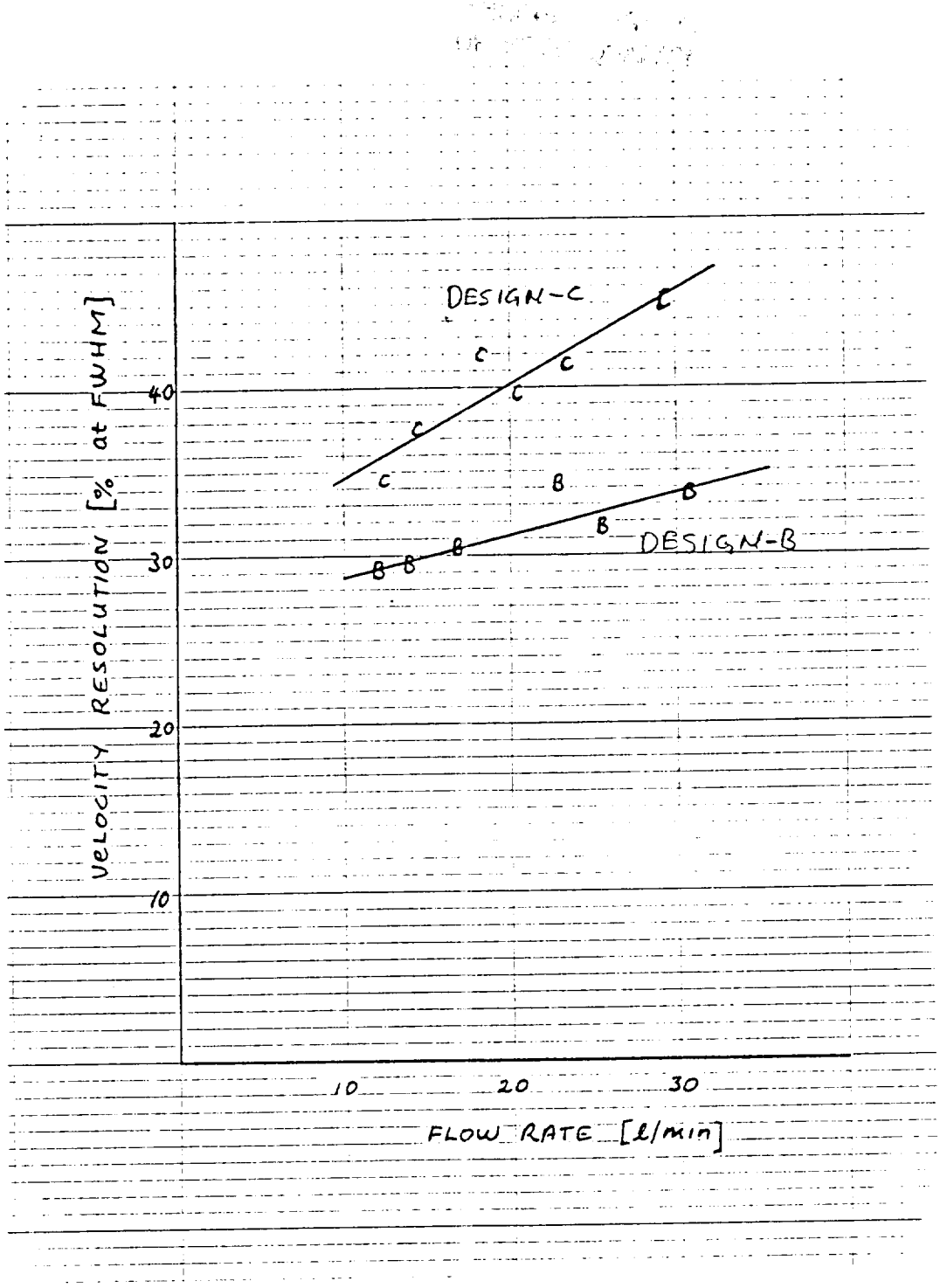

Figure 7.9

VELOCITY RESOLUTION - PEAK WIDTH AT HALF PEAK HEIGHT FOR DESIGNS C AND B PLOTTED AGAINST FLOW RATE.

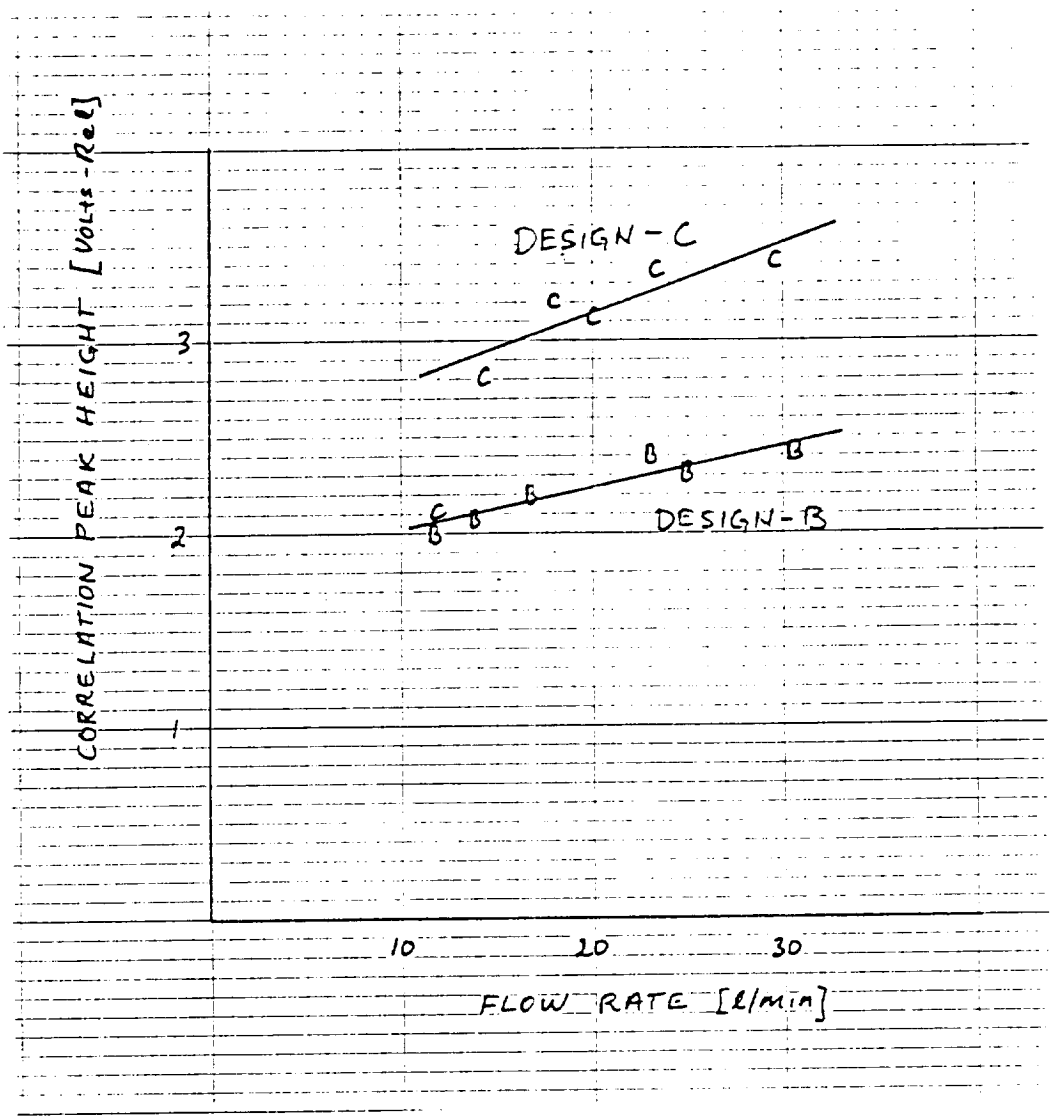

Figure 7.10

CORRELATION FUNCTION PEAK HEIGHT AS A FUNCTION OF FLOW RATE FOR DESIGNS B AND C.

correlation than design-B. This may be because design-C is responding more to the larger eddies (because of the longer electrode length) which are less likely to change between electrodes.

According to the test plan submitted to NASA, the flow "precision will be the dominant criteria" in selecting the best spool piece design and if necessary secondary results will be used. While the precision of all the designs is similar, design-A is selected as the most successful, based on precision and response time. this is followed in performance by design B and then design-C based on the potential for higher resolution with design-B.

7.1.3 Response to Step and Ramp Changes

The calibration tests were performed to indicate the response to ramp and step changes. The step change response was as expected and involves the correlation sweep rate and the number sweep cycles set for exponential smoothing.

Following step change the new cross correlation peak grows while the original peak diminishes. The process occurs at an exponential rate with a time constant equal to the correlation cycle time multiplied by the number of cycles selected for smoothing. Once the height of the new peak exceeds the original one the peak follower begins to track it by moving towards it in incremental steps. One time division increment is passed each correlation cycle. Since there is an inverse relation between time and flow rate the response is also an inverse relationship with rate dependent on the step change magnitude.

The overall response time was the sum of these delays for correlator configuration used. The overall response time constant was typically 8 seconds for design-A and 20 seconds for designs-B and C. If necessary, these time constants could have been reduced to negligible levels with a precision trade off. Options on the correlator provide for exponential smoothing adjustment and the elimination of the median peak follower to improve response time.

Response to ramp changes were as expected from the above discussion.

7.1.4 Transformer Oil Tests

Tests with transformer oil were made using an early spool piece prototype with a slightly different geometry. A diagram of the design is shown in Figure 7.11. Figure 7.12 shows a set of correlograms from transformer oil that demonstrate the application. Figure 7.12 shows the output voltage plotted against the turbine flow meter readings. This again demonstrates the linearity of the TEFM. Conversion of the TEFM readings to engineering units has not been done and does not provide any significant information.

7.2 Laboratory Cryogenic Tests

Several problems were encountered with the laboratory set up that prevented observation and analysis of triboelectric signal from single phase liquid nitrogen. These problems are known to originate from three basic causes: a) microphonics, b) two phase nitrogen flow and C) flow at low velocity.

Microphonics is caused by vibrations around the electrode assembly. Microphonics from other parts of the spool piece/preamplifier assembly were eliminated in the final design. It has been found that because of the construction of the two electrodes they respond in exactly the same way to vibration. This results in the same noise being generated. The special common mode rejection (CMR) feature of the correlator is able to correct for this effect and will be demonstrated in Section 7.3.

Two phase flow caused by bubble formation outside the dewars and bubble saturation masked any attempt to detect the true triboelectric signal. Attempts were made to reduce bubble formation outside the dewar by precooling as much external pipe work as possible. Prevention of bubbles caused by cavitation could not be ensured. Problems were also caused by nitrogen gas saturation after passing the liquid between the dewars. This gave rise to high frequency signals caused by the collapsing of these bubbles about the

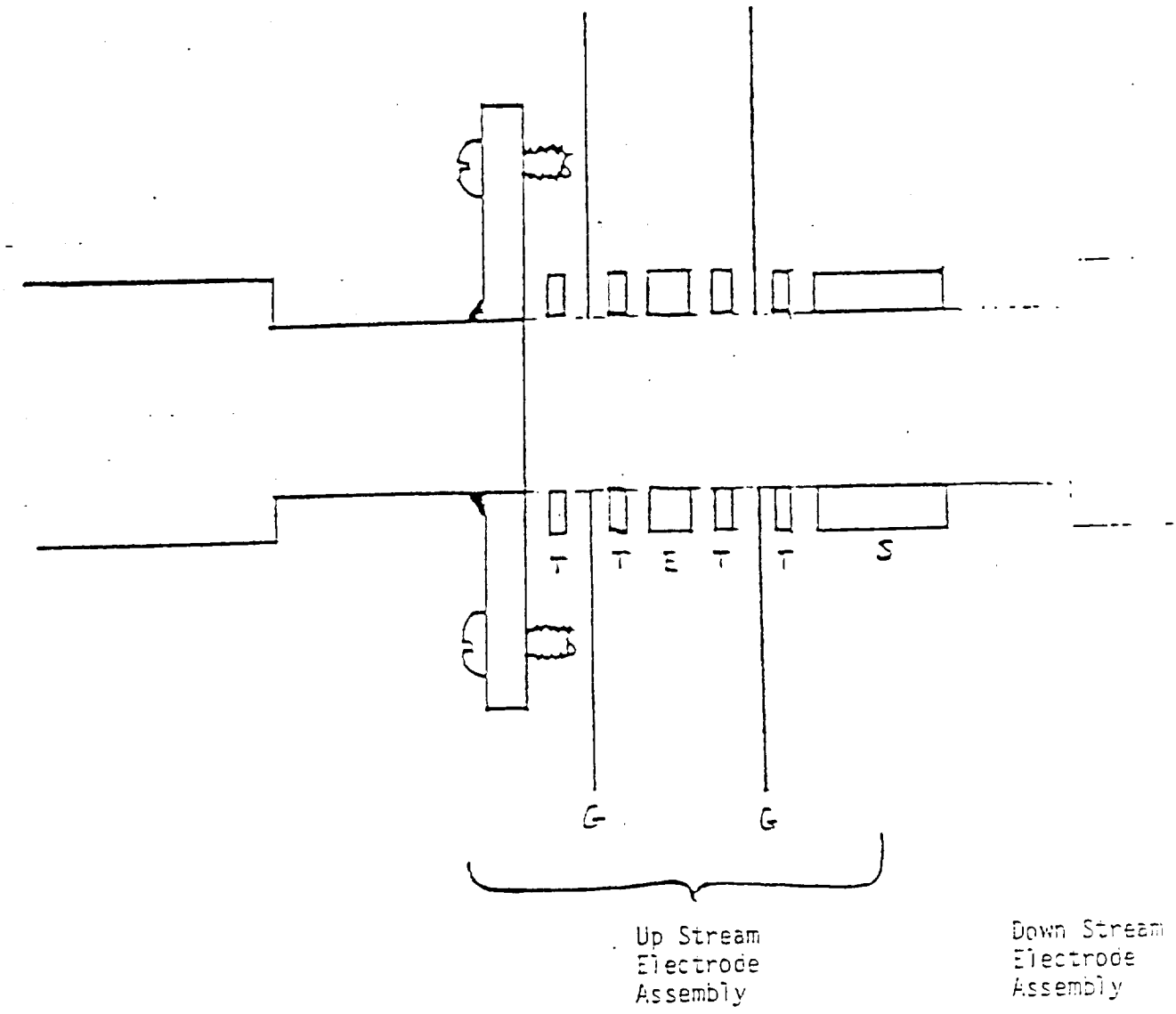

Figure 7.11

DIAGRAM OF THE EARLY PROTOTYPE DESIGN TESTED
WITH TRANSFORMER OIL

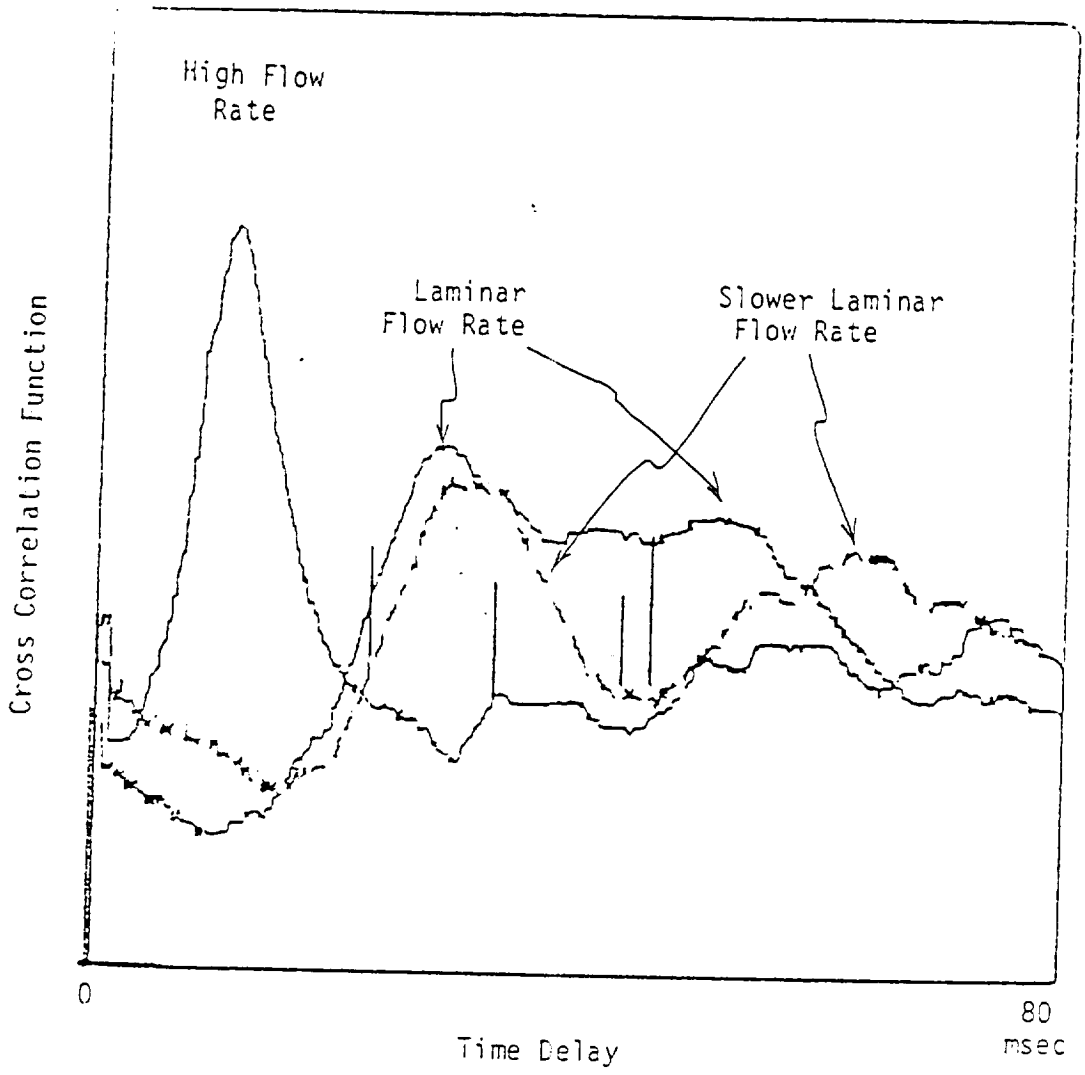

Figure 7.12

CORRELOGRAMS PRODUCED BY THE TEFM USING TRANSFORMER OIL FLOWING THROUGH AN EARLY PROTOTYPE DESIGN (FIG. 7.10)

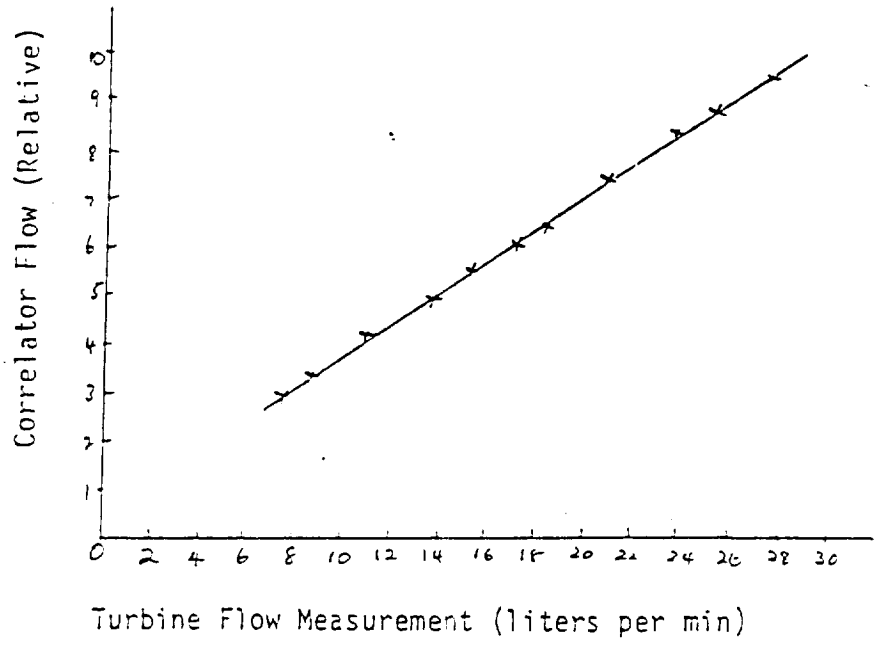

Figure 7.13

TEFM MEASUREMENT IN RELATIVE UNITS (VOLTS FROM CORRELATOR) PLOTTED AGAINST THE TURBINE FLOW METER READINGS

electrodes and between the electrodes such that the signals would not correlate.

The existence of bubbles does not necessarily prevent the use of the TEFM. Bubbles give rise to large signals from the electrodes which are cross correlated provided the bubbles do not change in form from one electrode to the other. Bubble velocity, however, may not equal liquid velocity. Figure 7.14 shows the response of the TEFM compared with the turbine flow meter during the presence of bubbles. Parts of the piping were left uninsulated to

be sure that bubbles were present. The non linearities shown in Figure 7.14 are probably due to the effects of larger bubbles on the turbine flow meter.

7.3 Cryogenic Tests - Depot

Arrangements were made to test the TEFM at a liquid nitrogen depot that had a large supply of subcooled liquid. A more compact and portable spool piece test apparatus was used as described in Section 6.2.2.

The possibility of bubbles could not be eliminated. However, from experience in observing known bubble-derived signals the presence of bubbles seemed to be less likely. Shortly after beginning the LN_2 flow reasonable cross correlation was detected which faded as the apparatus became sufficiently cooled. Hence this temporary cross correlation is considered to be caused by bubbles rather that triboelectric signals.

The most significant problem was caused by microphonic noise generated from around the electrodes. This was always common mode (CM) and was readily eliminated by the cross correlator common mode rejection (CMR) facility. Figure 7.15 shows an example of CM noise from each electrode. These signals are remarkably similar leading to the suspicion that there was cross talk between the signals before the high impedance part of the preamplifier. This possibility was eliminated by various tests which ensured isolation. The two preamplifier channels were eventually separated on different circuit boards. No triboelectric or non-common mode signals can be observed on these signals.

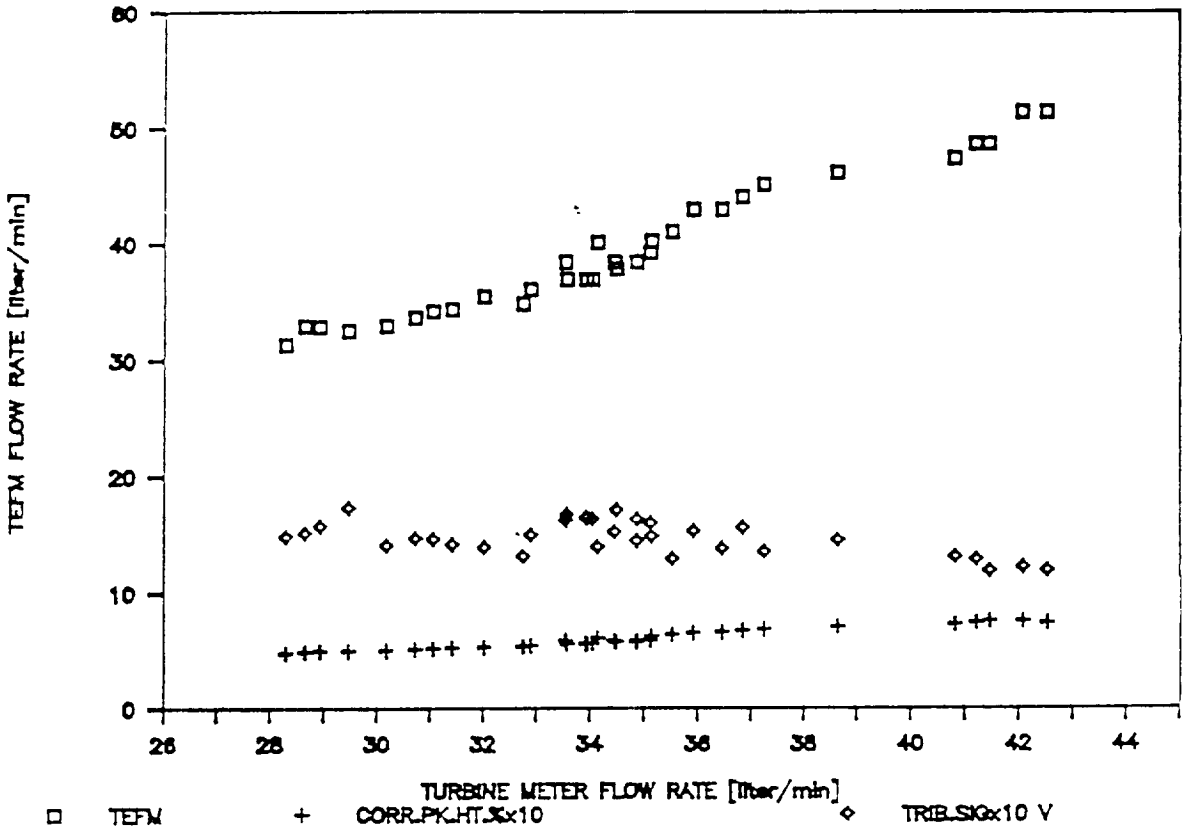

Figure 7.14

RESPONSE OF THE TEFM (DESIGN A) TO LIQUID NITROGEN CONTAINING BUBBLES

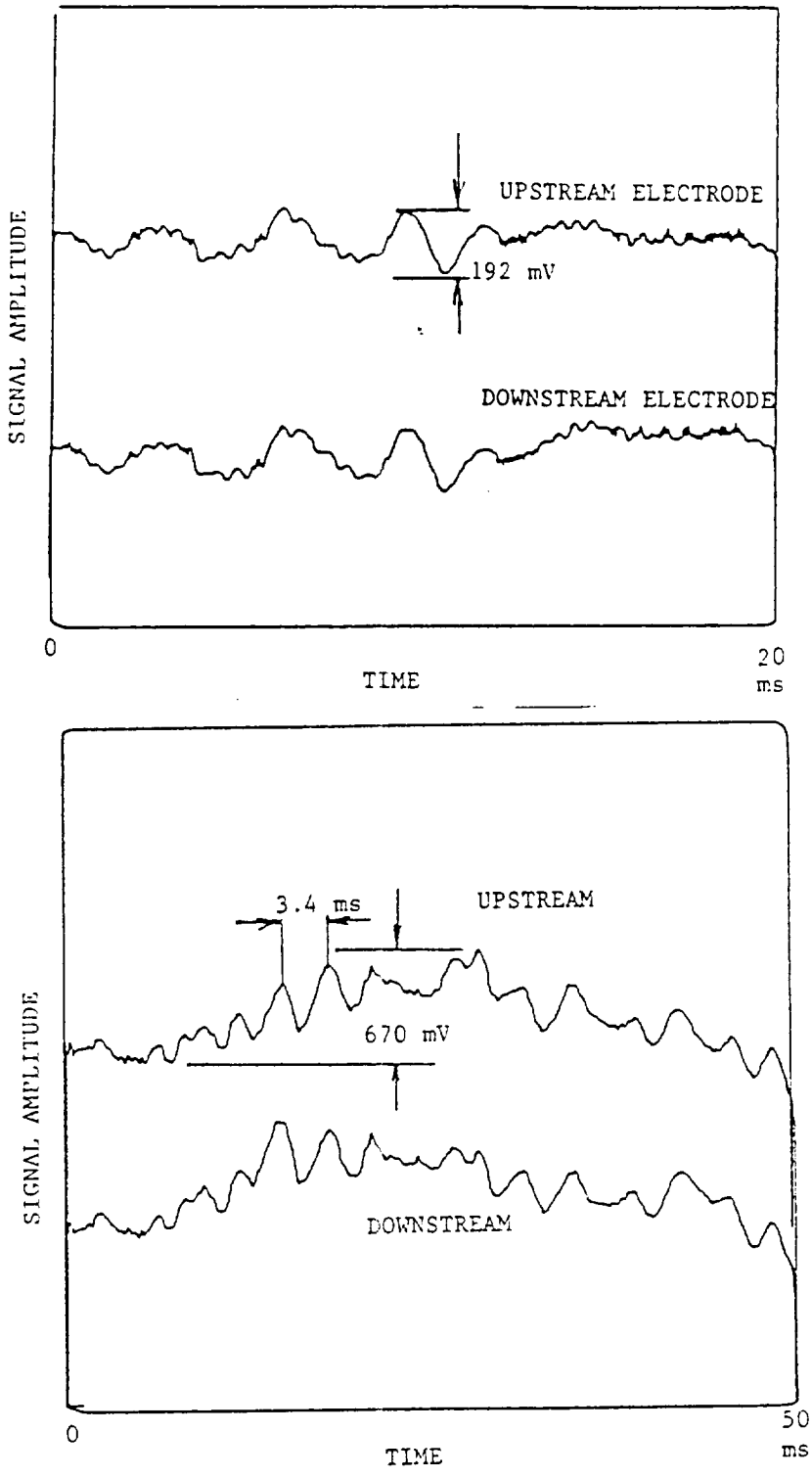

Figure 7.15

EXAMPLE OF COMMON MODE SIGNALS FROM SPOOL PIECE DESIGN A USING DEPOT LIQUID NITROGEN

Demonstration of the effect of common mode noise is shown in Figure 7.16(a). This shows the auto correlation function produced by the noise. Figure 7.16(b) shows how the CMR successfully eliminates the auto correlation function. No evidence of cross correlated (or non-CM) signal can be seen.

Figure 7.17 shows the electrode signal which contains harmonic microphonic noise in the presence of bubble generated noise. The cross correlation function shown was obtained using the CMR and the cross correlation peak can be clearly seen without any harmonic auto correlation features. The poor shape of the peak is due to the properties of the bubbles. This was typical of the signals shortly after starting the flow of liquid nitrogen.
The above results were obtained with the spool piece as close as possible to the LN_2 tank outlet. It was considered that the absence of observable triboelectric signal was because not enough time was allowed for the liquid to acquire and mix triboelectric charge. To test this, an extra one meter length of precooled pipe was installed between the spool piece and the LN_2 source. This pipe was galvanized steel and had a rough inner surface to aide in charge generation. This did not give rise to observable triboelectric signal. More harmonic microphonic noise was generated that showed frequency components consistent with resonance of acoustic vibrations within the pipe section.

It is estimated that any existing triboelectric noise in LN_2 at these flow rates must be not greater than approximately 1 mV (peak to peak) before amplification. This is when microphonic noise ranges about 5 mV (peak to peak) before amplification. Thus testing of the TEFM has not clearly identified any usable triboelectric noise against the background of other noise sources in liquid nitrogen. It should be noted that with such high signal to noise ratios, multibit correlation would be more effective in extracting any signal. The correlator used has the facility for two bit operation but required a different signal conditioning module design for operation. Two bit operation was thought to be unnecessary during the design phase following encouraging tests with freon.

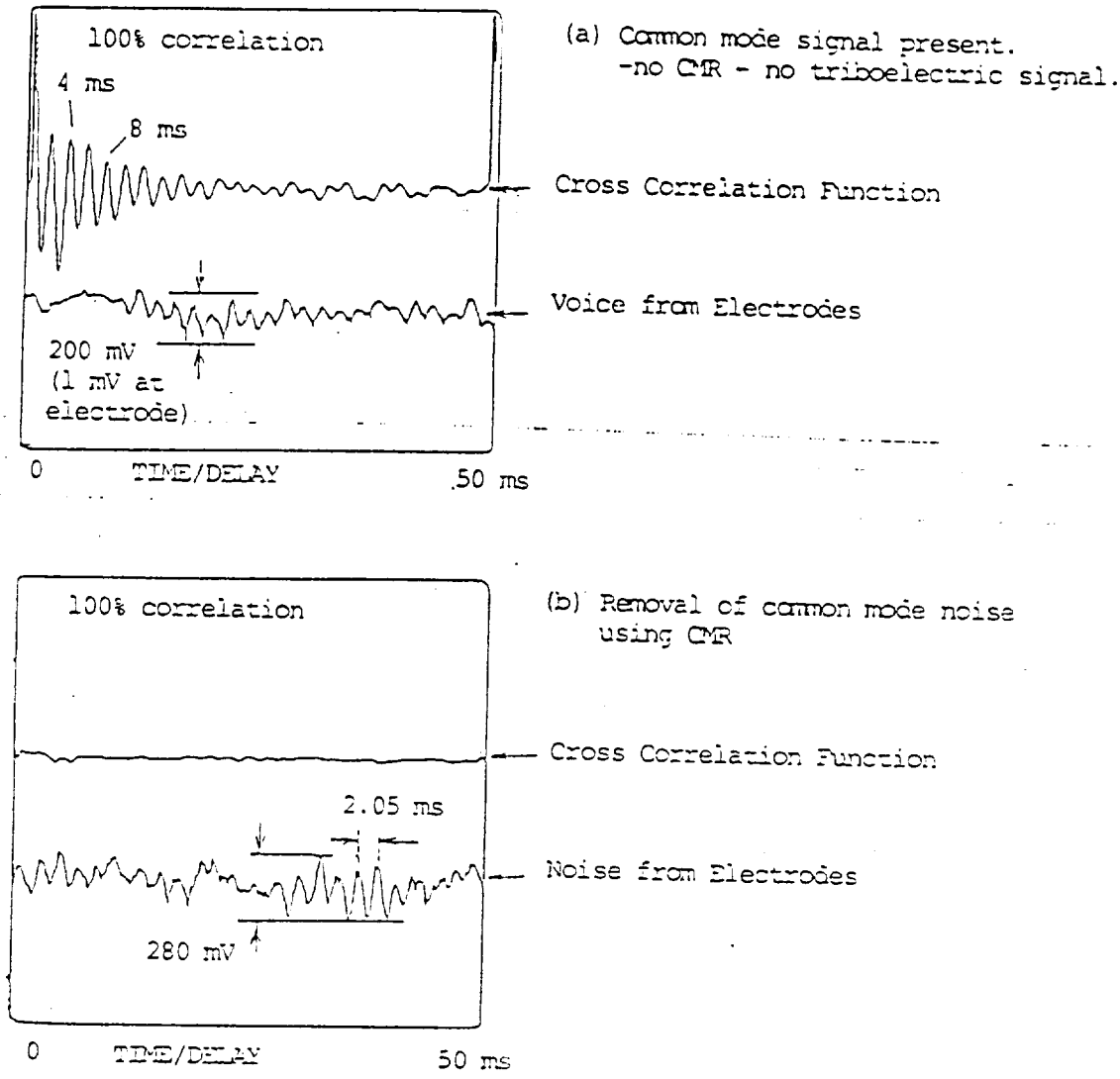

Figure 7.16

EFFECT OF COMMON MODE NOISE AND THE COMMON MODE NOISE REJECTION FACILITY

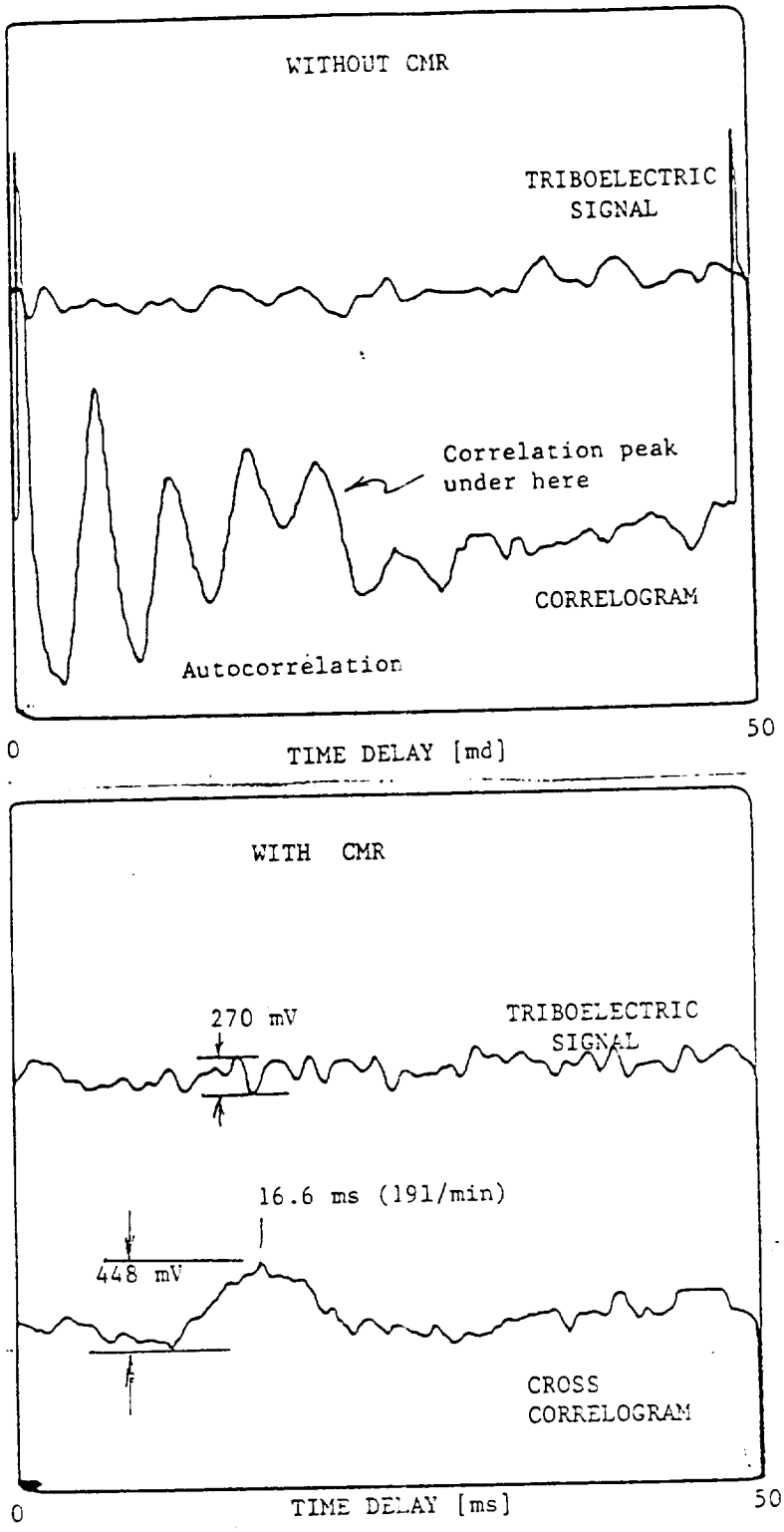

Figure 7.17

EFFECT OF COMMON MODE NOISE REJECTION FACILITY IN EXTRACTING CROSS CORRELATED SIGNAL

8.0 CONCLUSIONS

The feasibility of using the triboelectric for measuring cryogenic fuel flow has not been reliably demonstrated with liquid nitrogen. Two phase flow and microphonics in the various test loops prevented conclusive measurement of any single phase, tribo-generated charge. This result does not rule out the TEFM for application to liquid oxygen and liquid hydrogen at SSME flow rates. Two conclusions follow:

1) Liquid nitrogen does not generate significant triboelectric charge for flow rates up to 55 l/min.
2) There was insufficient turbulence upstream of the TEFM.

Liquid oxygen and hydrogen are expected to be more reactive and have a greater potential for charge generation. In the SSME, there is a considerable source of turbulence to generate charge.

Three flow meter spool piece designs were developed and delivered that operated well water, transformer oil and liquid freon. Tests enabled design features to be tested and a confirmation of general understanding of the technique.

The triboelectric signal has a $^{1}/f$ frequency spectrum. Pre-whitening of this signal improves precision. Precision is improved with a broad and even frequency distribution. Another way of improving band width is to reduce the axial length of the electrode which does not reduce the signal strength.

The degree of cross correlation between two signals is indicated by the correlation function peak height. The degree of correlation improves as the electrode spacing is reduced. This leads to a faster response, but has lead to a broader peak width. The reason for this is thought to be due to lower frequency cut off for ac signal coupling. As the separation and/or the lower frequency cut off is reduced, there is more chance that both electrodes lie within the same polarity of charge which leads to a broader peak. Hence, as the electrode spacing is reduced, the lower frequency cut off must be

increased. Otherwise, close electrodes are more desirable because they provide better correlation and faster response time.

The response of the TEFM is linear for liquids tested and is expected to be always linear because of the constant shape of the flow velocity profile. A small gauge factor must be determined for each design to account for3H this flow profile. Flow rate precision between .3 and .4 l/min (approximately 1%) were measured for liquid freon.

The common mode rejection facility of the cross correlator was successful in eliminating common mode noise such as microphonics. This is expected to be an essential feature of any future application to the SSME. Further techniques can be developed to reduce the generation of noise by changing the number of electrodes and/or their design. Extra electrodes could be used to assist in noise elimination.

9.0 RECOMMENDATIONS

From experience with this contract and other applications of the triboelectric technique for flow measurement. The most important test is to determine how much charge is generated by the fluid at its normal operating flow rate. Provided usable charge is generated, then it is highly probable that the technique will be successful.

Use of liquid nitrogen is less desirable than liquid oxygen which can be safely used in most laboratories. Further testing should be made to determine whether usable triboelectric signal is generated by liquid oxygen and liquid hydrogen. This should also be done with similar materials to those used in the SSME because these may generate different amounts of charge due to their location in the triboelectric series. Should such signal exist, then further work can be done to develop a method of reducing microphonic noise from the electrodes.

The amount of signal (ac and streaming potential) should also be estimated at the expected SSME flow rates. Testing at 10% of this flow rate should allow this estimation and should be done for liquids oxygen, hydrogen and nitrogen. To allow for further testing the current spool pieces should be modified to allow for higher pressure operation as required. Two of the spool pieces (designs A and B) were pressure tested to 220 PSI. Higher flow rate testing will take advantage of the ability of the cross correlator to operate at higher speeds (table 5.1). Should there be insufficient signal generation in liquid hydrogen and oxygen then a means of introducing charge should be investigated. Such methods include the use of electric fields or ionizing radiation.

The current signal conditioner/correlator occupies only two small circuit boards. For application to the space shuttle this size can be further reduced by at least half using hybridization and programmable logic gate arrays (PLGA). Prototypes using PLGA's for the cross correlator for different applications indicate a considerable reduction in chip count. Multilayer circuit board construction will also help to reduce the size of the electronics package to be more compatible with the space shuttle environment.

REFERENCES

1. More, A.D.; Electrostatics and its Applications, Wiley, 1973.

2. Cheremisinoff, N.P.; Gupta, R.; Handbook of Fluids in Motion, Butterworths, 1983.

3. Philip, J.; Charge Generation During Flow of a Hydrocarbon Liquid through MICRO-porous Media, Ph.D. thesis, John Hopkins University, 1966.

4. Ishibash, R.; Hanaoka, R.; High-field Electronic Conduction in Liquid Nitrogen, IEEE Trnas. Elec. Insul. Vol EI-17 No 6, December 1982.

5. Awschalom, D.D.; Milliken, F.P.; Schwarz, K.W.; Properties of Superfluid Turbulence in a Large Channel, Physical Review Letters, Vol 53 No. 14, October 1984.

6. Varga, I.K.; The Tribo-electric Effect of Liquid Flow and its Applications, Australian Dept. of Defense report ERL-0137-TR, July 1980.

7. Coulthard, J. Cross Correlation Flow Measurement - A History and the State of the Art, Meas, and Cont, Vol 16, June 1983.

8. Beck, M.S.; Drane, J.; Plaskowski, A.; Wainwright, N.; Particle Velocity and Mass Flow Measurement in Pneumatic Conveyors, Powder Technology, Vol. 2, 1968/69.

9. Beck, M.S., Coulthard, J., Hewitt, P.J., Sykes, D., Flow Velocity and Mass Flow Measurement Using Natural Turbulence Signals, International Conference on Modern Developments in Measurement, London 1972.

10. Green, R.G., Foo, S.H.; Solids Mass Flow Measurement in Pneumatic Pipelines, Bulk Solids Handling, Vol. 2 No. 4, December 1982.

11. American Patent No. 4,506,541, March 26, 1985.

12. King, P.W.; Mass Flow Measurement of Conveyed Solids by Monitoring of Intrinsic Electrostatic Noise Levels, Proc. 2nd International Conference on the Pneumatic Transport of Solids in Pipes, Surrey University UK, 1973.

13. Bendat, J.S.; Pierson, A.G.; Engineering Applications of Correlation and Spectral Analysis, John Wiley, 1980.

14. Eldon, J.A.; Digital Correlators Suit Military Applications, (TRW LSI Products Div.), EDN, August 1984.

15. Cooper, G.; McGillen, C.; Probabilistic Methods of Signal Analysis, Holt, Rinehart and Winston Inc, 1971.